International Journal of Fatigue 67 (2014) 38–54

Contents lists available at ScienceDirect

International Journal of Fatigue

journal homepage: www.elsevier.com/locate/ijfatigue

Four stress analysis strategies to use the Modified Wöhler Curve Method to perform the fatigue assessment of weldments subjected to constant and variable amplitude multiaxial fatigue loading

Luca Susmel

Department of Civil and Structural Engineering, The University of Sheffield, Mappin Street, Sheffield S1 3JD, UK

ARTICLE INFO

Article history:
Received 17 August 2013
Received in revised form 28 November 2013
Accepted 4 December 2013
Available online 12 December 2013

Keywords:
Welded joints
Multiaxial fatigue
Critical plane
Variable amplitude loading

ABSTRACT

The present paper investigates the different ways of using the Modified Wöhler Curve Method (MWCM) to perform the fatigue assessment of steel and aluminium welded joints subjected to in-service variable amplitude (VA) multiaxial load histories. Thanks to its specific features, the above critical plane approach can efficiently be applied in terms of both nominal, hot-spot, and local quantities, that is, by using any of the stress analysis strategies suggested by the Design Recommendations of the International Institute of Welding (IIW). The MWCM can efficiently be used also along with the so-called Theory of Critical Distances applied in the form of the Point Method (PM). The accuracy of the different formalisations of the MWCM investigated in the present paper was systematically checked against a large number of experimental results taken from the literature and generated by testing, under VA biaxial nominal loading, welded samples having different geometries. Such a systematic validation exercise allowed us to prove that our multiaxial fatigue criterion is successful in designing welded joints against VA multiaxial fatigue, this holding true independently from both definition adopted to calculate the necessary stress quantities and complexity of the assessed load history.

1. Introduction

To design un-cracked welded components of both steel and aluminium against fatigue, the available Design Codes and Recommendations [1–3] allow structural engineers to perform the stress analysis according to three different strategies, i.e., in terms of either nominal, hot-spot, or local stresses. In more detail, nominal stresses are suggested as being calculated according to classical continuum mechanics, without explicitly modelling the stress concentration phenomena at the weld toe. All the calculations are done by assuming that the designed material obeys a linear-elastic constitutive law and the effects of macro-geometrical features as well as the presence of concentrated loadings must always be taken into account [3,4].

Hot-spot stresses are instead used either when a reference design curve is not available for the specific welded detail being assessed, or when a nominal section cannot unambiguously be defined due to the complexity of the geometry of the component being designed. Hot-spot stress quantities can be determined from conventional linear-elastic finite element (FE) models as well as by directly measuring the local strains through strain gauges attached, in the vicinity of the assumed crack initiation locations, to the surface of the welded component being assessed [3–5]: as soon as the linear-elastic stress is known either at two or at three superficial reference points, the structural stress is directly extrapolated to the weld toe at the hot spot. Finally, according to the IIW [3] the stress analysis can be performed also in terms of local quantities, where the critical stress states are suggested as being determined by rounding either the weld toe or the weld root with a reference radius having length equal to either 1 mm or to 0.05 mm [4].

Other than those approaches suggested by the available Standard Codes and Recommendations as being adopted in situations of practical interest, examination of the state of the art shows that in recent years many different attempts have been made to devise alternative design techniques taking full advantage of local quantities. Amongst the different approaches which have been proposed so far, and somehow validated through experimental results, certainly the N-SIF approach [6,7], the Strain Energy Density parameter [8,9], and the Theory of Critical Distances [10,11] deserve to be mentioned explicitly.

As far as multiaxial fatigue loadings are concerned, apart from those simplified methods recommended by some design codes [3,12], examination of the state of the art shows that the most accurate estimates are obtained by using those critical plane approaches specifically devised to post-process either structural or local quantities [12–17].

E-mail address: l.susmel@sheffield.ac.uk

0142-1123/$ - see front matter © 2013 Elsevier Ltd. All rights reserved.
http://dx.doi.org/10.1016/j.ijfatigue.2013.12.001

Nomenclature

a, b, α, β	constants in the MWCM's calibration equations
f_Σ	frequency of the axial stress component
f_T	frequency of the torsional stress component
$f(R_{CP})$	enhancement factor
$f(\tau)$	shear stress enhancement factor
k	negative inverse slope of the uniaxial fatigue curve
k_0	negative inverse slope of the torsional fatigue curve
k_τ	modified Wöhler curve's negative inverse slope
m_τ	modified Wöhler curve's negative inverse slope in the high-cycle fatigue regime
n	number of cycles
t	time
D_{cr}	critical value of the damage sum
D_{tot}	damage sum
F	ratio between f_Σ and f_T
$M\text{-}D_V$	multiaxial critical distance
N_f	number of cycles to failure
$N_{f,e}$	estimated number of cycles to failure
N_{kp}	number of cycles to failure defining the position of the knee point
N_A	reference number of cycles to failure
$Oxyz$	system of coordinates
P_S	probability of survival
R	load ratio
R_{CP}	critical plane load ratio ($R_{CP} = \sigma_{n,min}/\sigma_{n,max}$)
T	time interval
T_σ, T_τ	scatter ratio of the stress amplitude for 90% and 10% probabilities of survival
δ	out-of-phase angle
ρ_w	critical plane stress ratio
$\rho_{w,lim}$	limit value for the critical plane stress ratio
$\sigma_i(t)$	instantaneous value of the normal stress ($i = x, y, z$)
$\sigma_n(t)$	instantaneous value of the stress perpendicular to the critical plane
$\sigma_{n,a}$	amplitude of the stress perpendicular to the critical plane
$\sigma_{n,m}$	mean stress perpendicular to the critical plane
$\sigma_{n,max}$	maximum stress perpendicular to the critical plane
$\sigma_{n,min}$	minimum stress perpendicular to the critical plane
τ_a	maximum shear stress amplitude
$\tau_{ij}(t)$	instantaneous value of the shear stress ($i, j = x, y, z$)
τ_m	mean shear stress
$\tau_{MV}(t)$	instantaneous value of the shear stress resolved along the maximum variance direction
$\tau_{MV,max}$	maximum shear stress resolved along the maximum variance direction
$\tau_{MV,min}$	minimum shear stress resolved along the maximum variance direction
$\Delta\sigma_A$	range of the reference normal stress at N_A cycles to failure
$\Delta\sigma_n$	normal stress range relative to the critical plane
$\Delta\tau$	shear stress range relative to the critical plane
$\Delta\tau_A$	range of the reference shear stress at N_A cycles to failure
$\Delta\tau_{Ref}$	reference shear stress range relative to the critical plane
$\Delta\Sigma_i$	range of the uniaxial nominal stress during the i-th loading cycle
ΔT_i	range of the torsional nominal stress during the i-th loading cycle

Turning back to uniaxial nominal situations, the three types of stress analysis mentioned above can be used also to perform the fatigue assessment of weldments subjected to VA fatigue loading [4], in such circumstances [3,4] cumulative fatigue damage being usually calculated according to the linear rule due to Palmgren [18] and Miner [19]. The most tricky aspect behind the use of the above classical rule to design real welded components against VA fatigue is that the critical value of the damage sum is seen to vary in the range 0.01–10 [20], its average value being equal to 0.45 for welded steel and to 0.27 for welded aluminium [21]. Therefore, according to the above experimental evidence, the IIW suggests performing the fatigue assessment under VA fatigue loading by adopting a critical value of the damage sum invariably equal to 0.5 [3].

From a fatigue design point of view, the situation becomes much more complex when VA multiaxial load histories are involved, since, given the welded detail, the critical value of the damage sum is seen to vary as the degree of multiaxiality and non-proportionality of the investigated load history varies [14,21–23]. For instance, by performing an accurate experimental investigation, Sonsino and Kueppers [14] have observed that, for their tube-to-plate steel welded joints subjected to Gaussian Spectra with sequence length of $5{\cdot}10^4$ cycles, the critical value of the damage sum was equal to 0.08 under VA pure bending, to 0.38 under VA pure torsion and to 0.35 under in-phase and 90° out-of-phase VA combined bending and torsion.

In this complex scenario, aim of the present paper is to show, through a systematic validation exercise based on experimental results taken from the literature, that the MWCM can successfully be applied in terms of either nominal, hot-spot, or local stresses to perform the fatigue assessment of both steel and aluminium welded joints subjected to in-service VA multiaxial fatigue loading.

2. Stress components relative to the critical plane and cycle counting under variable amplitude multiaxial fatigue loading

The MWCM is a bi-parametrical critical plane approach whose formalisation takes as a starting point the assumption that fatigue damage, under both variable and constant amplitude (CA) loading, reaches its maximum value on that plane (i.e., the so-called critical plane) experiencing the maximum shear stress amplitude.

By initially focussing attention solely on the CA problem, examination of the state of the art shows that different definitions [24] can successfully be adopted to calculate the maximum shear stress amplitude, τ_a, the most simple one being that based on the use of the maximum chord concept [25]. Even if the classical definitions are seen to be successful in calculating τ_a, one of the most tricky aspects in using them to design real components against CA fatigue is that, in theory, the shear stress amplitude relative to any plane passing through the assumed critical point should be calculated, by determining *a posteriori* that plane on which the shear stress amplitude itself reaches its maximum value. Since this *modus operandi* can become extremely time-consuming when complex and long load histories are involved [26,27], in recent years we have made a big effort in order to device an alternative definition [24,28] based on the maximum variance concept [29]. The Maximum Variance Method (MVM) [28] postulates that the critical plane can be defined as that plane containing the direction (passing through the assumed critical point) that experiences the maximum variance of the resolved shear stress, $\tau_{MV}(t)$ – see Fig. 1a and b. From a practical point of view, the most remarkable peculiarity of the MVM is that, as soon as the variance and co-variance terms of the stress components at the critical location are known, the computational time required to determine the orientation of the critical plane does not depend on the length of the input load

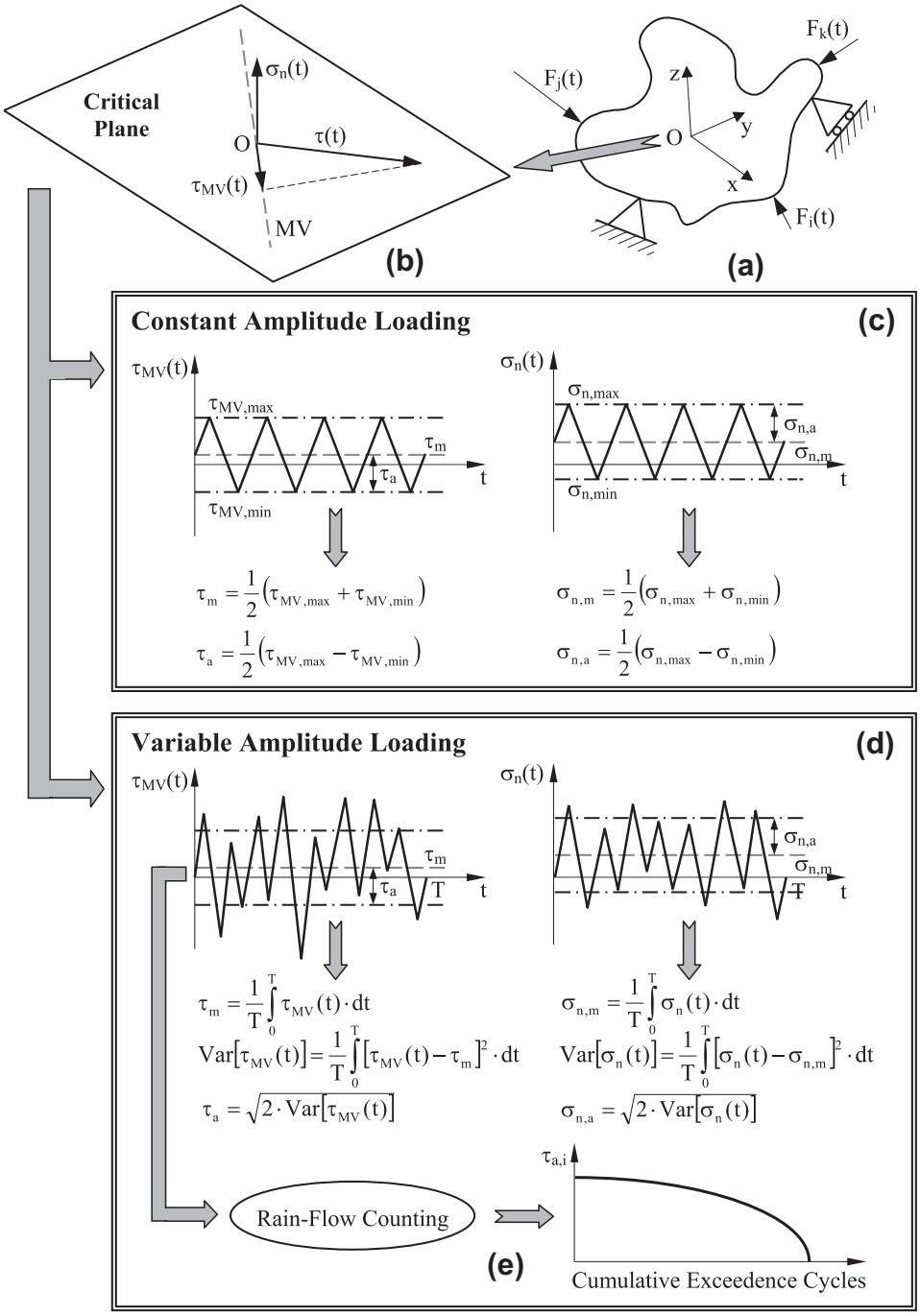

Fig. 1. Adopted definitions to calculate the amplitude and the mean value of the stress components relative to the critical plane under both constant and variable amplitude loading.

history being assessed [30]. Since the main features of the MVM have already been discussed in Refs [24,28,30] in great detail, by also investigating the different issues behind the numerical solution of the associated multi-variable optimisation problem [30], only the different definitions suitable for calculating the stress quantities relative to the critical plane under both constant and variable amplitude loading will briefly be reviewed in what follows.

Consider then a body subjected to a complex system of time-variable forces resulting in a time-variable multiaxial stress state at the assumed critical location (point O in Fig. 1a). According to the MVM [24,28,30], the critical plane is then the one containing that direction, MV, experiencing the maximum variance of the resolved shear stress, $\tau_{MV}(t)$ (Fig. 1b). It is worth recalling here that, by definition, the variance of a time-variable signal is the expected value of the square of the deviation of that signal from its mean value. According to the above definition, the variance of a time-variable signal gives a measure of the amount of variation of the signal itself within the two extremes defining the maximum range, the variance being obviously independent from the mean value of the considered signal.

This remark should make it evident that the above definition can be used to determine the orientation of the critical plane not only under CA, but also under VA multiaxial fatigue loading [31]. Turning back to the CA problem, if the body sketched in Fig. 1a is

initially assumed to be subjected to a system of cyclic forces resulting in a CA stress state at critical point O, as soon as the orientation of the critical plane is known (through the direction experiencing the maximum variance of the resolved shear stress), the amplitude, τ_a, and the mean value, τ_m, of the shear stress relative to the critical plane can directly be calculated as follows (Fig. 1c):

$$\tau_a = \frac{1}{2}(\tau_{MV,max} - \tau_{MV,min}) \tag{1}$$

$$\tau_m = \frac{1}{2}(\tau_{MV,max} + \tau_{MV,min}) \tag{2}$$

where $\tau_{MV,max}$ and $\tau_{MV,min}$ are the maximum and minimum value of $\tau_{MV}(t)$, respectively. As to the polarity of the shear stress, it is worth recalling here that the sign of the shear stress components have to be unambiguously and consistently assigned according to the convention being adopted. In a similar way, the amplitude, $\sigma_{n,a}$, and the mean value, $\sigma_{n,m}$, of the stress perpendicular to the critical plane, $\sigma_n(t)$, turn out to be (Fig. 1c):

$$\sigma_{n,a} = \frac{1}{2}(\sigma_{n,max} - \sigma_{n,min}) \tag{3}$$

$$\sigma_{n,m} = \frac{1}{2}(\sigma_{n,max} + \sigma_{n,min}), \tag{4}$$

$\sigma_{n,max}$ and $\sigma_{n,min}$ being the maximum and minimum value of $\sigma_n(t)$ during the loading cycle, respectively.

Assume now that the body of Fig. 1a is subjected to a complex system of time-variable forces resulting in a stress state at point O whose components vary randomly over the time interval [0,T]. According to the MVM [24,28,30], the critical plane can be determined also in such circumstances by directly locating that plane containing the direction, MV, experiencing the maximum variance of resolved shear stress $\tau_{MV}(t)$. As soon as the orientation of the critical plane is known, the mean value of the shear stress relative to the critical plane takes on the following value:

$$\tau_m = \frac{1}{T}\int_0^T \tau_{MV}(t)\cdot dt, \tag{5}$$

whereas the equivalent stress amplitude of the resolved shear stress is equal to [30]:

$$\tau_a = \sqrt{2\cdot \mathrm{Var}[\tau_{MV}(t)]}, \tag{6}$$

the variance of stress signal $\tau_{MV}(t)$ being:

$$\mathrm{Var}[\tau_{MV}(t)] = \frac{1}{T}\int_0^T [\tau_{MV}(t) - \tau_m]^2 \cdot dt \tag{7}$$

By following the same strategy as above, the equivalent amplitude and the mean value of normal stress $\sigma_n(t)$ take on the following values [30]:

$$\sigma_{n,m} = \frac{1}{T}\int_0^T \sigma_n(t)\cdot dt \tag{8}$$

$$\sigma_{n,a} = \sqrt{2\cdot \mathrm{Var}[\sigma_n(t)]}, \tag{9}$$

$\mathrm{Var}[\sigma_n(t)]$ being the variance of stress component $\sigma_n(t)$, i.e.:

$$\mathrm{Var}[\sigma_n(t)] = \frac{1}{T}\int_0^T [\sigma_n(t) - \sigma_{n,m}]^2 \cdot dt \tag{10}$$

For the sake of clarity, Fig. 1d graphically shows the meaning of the above definitions: the schematic charts of Fig. 1d should make it evident that the equivalent amplitudes of both resolved shear stress $\tau_{MV}(t)$ and normal stress $\sigma_n(t)$ are proportional to the amount of variation of the stress signals themselves. Another problem which can briefly be addressed here is the way of performing the cycle counting under VA uniaxial/multiaxial fatigue loading when the fatigue assessment is performed through the MWCM. In particular, since, as said above, under CA fatigue loading, the MWCM takes as its starting point the assumption that fatigue damage reaches its maximum value on the plane of maximum shear stress amplitude [24], it is logical to hypothesise that, under VA fatigue loading, resolved shear stress $\tau_{MV}(t)$ is the stress signal to be post-processed in order to efficiently count fatigue cycles. The cycle counting can directly be performed according to the classical Three-Point Rain Flow Method owing to the fact that, by definition, $\tau_{MV}(t)$ is a mono-dimensional quantity [31,32]: by so doing, from the counted shear stress cycles, the corresponding cumulative spectrum can directly be built and subsequently used to estimate the fatigue damage extent associated with the assessed load history (Fig. 1e).

To conclude, it is worth observing that the available Standard Codes and Recommendation usually address the problem of designing weldments against fatigue in terms of ranges. Accordingly, the ranges of the stress quantities relative to the critical plane can be calculated as follows:

$$\Delta\tau = 2\cdot\tau_a \tag{11}$$

$$\Delta\sigma_n = 2\cdot\sigma_{n,a} \tag{12}$$

where the amplitudes of the two relevant stress components have to be calculated according to the definitions reviewed above, that is, by distinguishing between constant and variable amplitude situations.

3. The Modified Wöhler Curve Method to design welded connections against fatigue

In the present section the main features of the MWCM are briefly reviewed by specifically describing the way our multiaxial fatigue criterion is suggested as being used to perform the fatigue assessment of welded connections. The in-field procedures to be followed to estimate lifetime under both CA and VA multiaxial fatigue loading will be summarised by addressing the problem in its most general form, that is, independently of the strategy adopted to determine the relevant stress state at the assumed critical point. In the next Sections instead, the way of applying the MWCM along with both nominal stresses, hot-spot quantities, the reference radius concept, and the Theory of Critical Distances will be investigated in depth, by also showing the existing links, and the consequent implications, between the MWCM's *modus operandi* and the adopted definition to determine the stress state at the assumed critical location.

Turning back to the in-field usage of the MWCM, our criterion estimates the fatigue damage extent associated with the assessed load history through the ranges of the stress components relative to the critical plane, the combined effect of the shear and normal stress being taken into account by means of the following stress ratio [24,33]:

$$\rho_w = \frac{\Delta\sigma_n}{\Delta\tau} \tag{13}$$

The most relevant peculiarity of the above stress quantity is that, thanks to the way it is defined, ρ_w is seen to be sensitive to the degree of multiaxiality and non-proportionality of the stress state at the assessed critical point: for instance, ρ_w is equal to unity under uniaxial fatigue loading, whereas it is invariably equal to zero under torsion [24]. Intentionally, the critical plane stress ratio is instead insensitive to the presence of non-zero mean stresses: this suggests that ρ_w as defined above can be used solely to perform the fatigue assessment of weldments working in the as-welded condition, that is, in those circumstances in which, due to the residual stresses acting on the material in the vicinity of the weld bead, the presence of

superimposed static stresses can be neglected with little loss of accuracy [3,4,24]. With regard to the non-damaging effect of non-zero mean stresses in as-welded joints, it is worth recalling here that such an experimental evidence is a consequence of the fact that the residual stresses resulting from the welding process change the local value of the load ratio, $R = \sigma_{min}/\sigma_{max}$, so that, under high tensile residual stresses, the local value of R can become larger than zero also under nominal load ratios approaching -1. Accordingly, welded joints in the as-welded condition can accurately be designed against fatigue by simply using reference fatigue curves generated under R ratios larger than zero (usually, by setting $R = 0.5$ [3]), this holding true independently from the magnitude of the superimposed static stresses applied to the connection being assessed [3,4]. On the contrary, in stress relieved welded joints, the effect of non-zero mean stresses cannot be disregarded and the presence of superimposed static stresses is usually taken into account through appropriate enhancement factors [3,4,34], their in-field use being explained in the next Sections in great detail.Consider then an as-welded joint subjected to a system of external forces resulting, at the critical location, in a CA multiaxial stress state (Fig. 2a and b). By taking full advantage of the MVM [30], the direction, MV, experiencing the maximum variance of the resolved shear stress can directly be determined (Fig. 2c). As soon as the orientation of the critical plane is known, the corresponding ranges of the shear, $\Delta\tau$, and normal, $\Delta\sigma_n$, stress (Fig. 2d and e) allow stress ratio ρ_w to directly be estimated through definition (13) – Fig. 2f. The way the MWCM estimates fatigue lifetime under CA fatigue loading is summarised through the log–log modified Wöhler diagram sketched in Fig. 2g. This chart plots the shear stress range relative to the critical plane, $\Delta\tau$, against the number of cycles to failure, N_f. In more detail, through a systematic reanalysis of numerous data sets, it was proven [24,35,36] that, given the material, different fatigue curves are obtained in the above Modified Wöhler diagram as ratio ρ_w varies, such curves being characterised by different values not only of the negative inverse slope $k_\tau(\rho_w)$, but also of the reference shear stress range, $\Delta\tau_{Ref}(\rho_w)$, extrapolated at N_A cycles to failure (Fig. 2g). The schematic modified Wöhler diagram of Fig. 2g should make it evident that, as soon as shear stress range $\Delta\tau$ is known, lifetime can directly be estimated provided that the design curve for the investigated value of ratio ρ_w is defined unambiguously. Since the experimental fatigue curves which are usually available are those generated under both uniaxial ($\rho_w = 1$) and

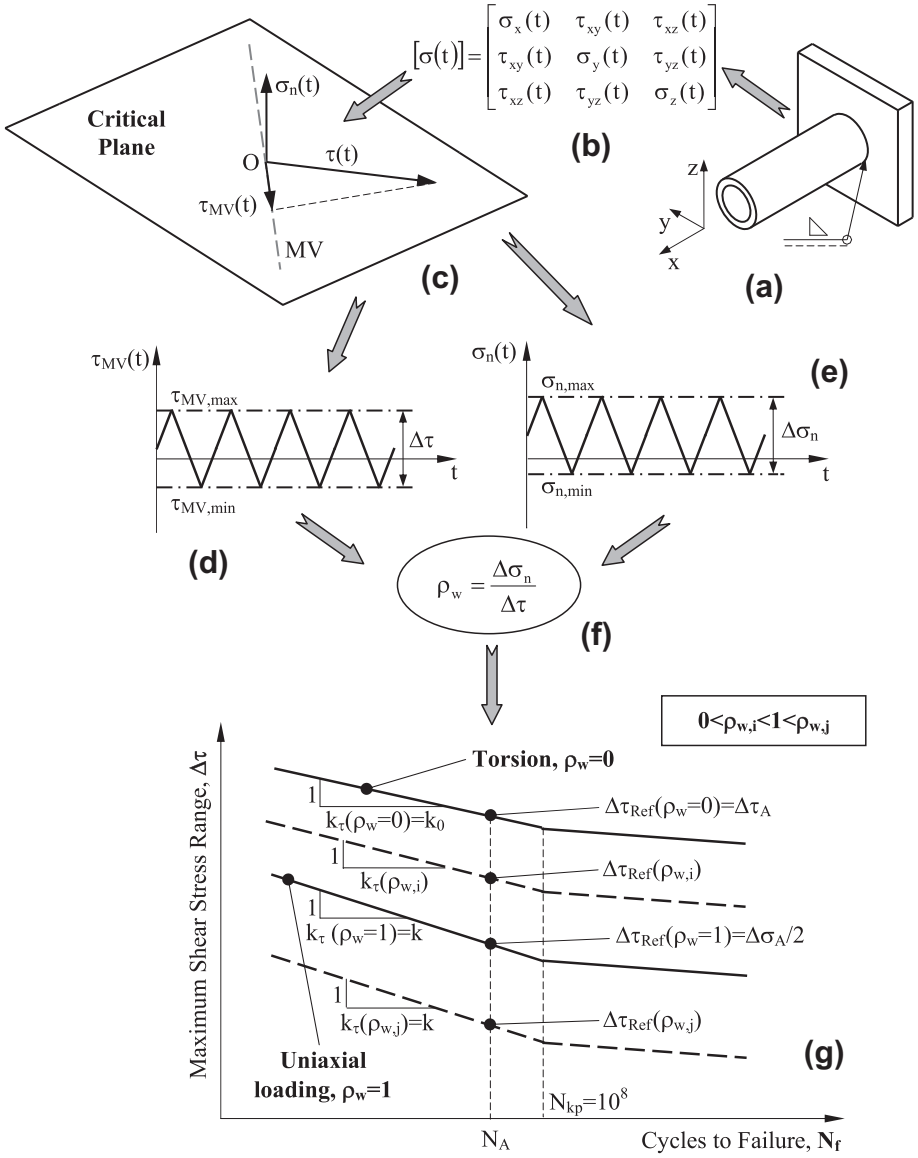

Fig. 2. Design against CA multiaxial fatigue loading and modified Wöhler diagram (g).

torsional ($\rho_w = 0$) fatigue loading, the position of any other modified Wöhler curve has to be estimated. By performing a systematic investigation based on a large number of experimental results, it was seen that accurate predictions can be made by defining the $\Delta\tau$ vs. ρ_w and k vs. ρ_w relationships through simple linear laws [24,36,37], i.e.:

$$k_\tau(\rho_w) = \alpha \cdot \rho_w + \beta \tag{14}$$

$$\Delta\tau_{Ref}(\rho_w) = a \cdot \rho_w + b \tag{15}$$

where a, b, α and β are material fatigue constants which can be determined experimentally. In particular, if the above constants are calibrated through the fatigue curves generated under uniaxial ($\rho_w = 1$) and torsional ($\rho_w = 0$) fatigue loading, respectively, they take on the following values [24]:

$$\alpha = k - k_0; \cdot\beta = k_0 \tag{16}$$

$$a = \frac{\Delta\sigma_A}{2} - \Delta\tau_A; b = \Delta\tau_A. \tag{17}$$

where k and k_0 are the negative inverse slopes of the uniaxial and torsional fatigue curve, respectively, whereas $\Delta\sigma_A$ and $\Delta\tau_A$ are the ranges of the corresponding reference stresses extrapolated at N_A cycles to failure (Fig. 2g).

It is worth observing here also that the range of the reference shear stress defining those modified Wöhler curves to be used to estimate fatigue lifetime under a ρ_w ratio larger than $\rho_{w,lim}$ is assumed to be constant and equal to $\Delta\tau_{Ref}(\rho_{w,lim})$, such a threshold value being determined as [24]:

$$\rho_{w,lim} = \frac{\Delta\tau_A}{2\Delta\tau_A - \Delta\sigma_A} \tag{18}$$

This assumption was made to take into account the experimental evidence that, under high values of ratio ρ_w, the use of the MWCM as formulated above resulted in estimates that were seen to be characterised by an excessive level of conservatism [24,38,39]. Such an high degree of conservatism was ascribed to the fact that, when critical planes experience large values of ratio ρ_w, fatigue damage is non longer solely shear stress governed. Accordingly, the use of the conventional critical plane approach as it stands is no longer justified, so that correction (18) was introduced in order to better take into account the contribution to the overall fatigue damage of the stress perpendicular to the critical plane [39].

Another important aspect which deserves to be discussed in great detail here is the way the k vs. ρ_w relationship, Eq. (14), is suggested as being defined to specifically design weldments against fatigue. In more detail, the negative inverse slope of modified Wöhler curves is recommended to be estimated as follows (Fig. 2g):

$$k_\tau(\rho_w) = [k - k_0] \cdot \rho_w + k_0 \quad \text{for } \rho_w \leqslant 1 \text{ and } N_f \leqslant N_{kp} \tag{19}$$

$$k_\tau(\rho_w) \equiv k \quad \text{for } \rho_w > 1 \text{ and } N_f \leqslant N_{kp} \tag{20}$$

N_{kp} being the number of cycles to failure that defines the position of the knee point. For $N_f > N_{kp}$ instead, the slope of the Modified Wöhler Curves under CA loading is suggested, as recommended by Sonsino [34], to be taken invariably equal to 22, this holding true independently from the actual value of the ρ_w ratio relative to the critical plane under investigation. With regard to the above hypothesis, it is important to recall here that, under axial loading, the IIW [3] recommends to take the knee point at $N_{kp} = 10^7$ cycles to failure, whereas under torsional loading at $N_{kp} = 10^8$ cycles to failure. Owing to the fact that the MWCM is a shear stress based criterion, to simplify the formalisation of the method itself, the knee point is suggested as being taken, independently from the degree of multiaxiality and non-proportionality of the assessed stress state, always at 10^8 cycles to failure [40].

The last relevant aspect which deserves to be commented here is the hypothesis that the negative inverse slope is constant and invariably equal to k under ρ_w values larger than unity – see Eq. (20). In particular, such an hypothesis is derived from the experimental evidence that, independently of the complexity of the load history damaging the welded detail being assessed, in general, the slope of the corresponding Modified Wöhler curve is never seen to be lower than the one of the uniaxial fatigue curve (having ρ_w equal to unity) [40].

Turning back to the way of performing the fatigue assessment according to the MWCM, after estimating, through Eqs (14) and (15), the modified Wöhler curve for the specific value of the ρ_w ratio characterising the critical plane being investigated, the number of cycles to failure can directly be calculated by using the following trivial relationship:

$$N_{f,e} = N_A \cdot \left[\frac{\Delta\tau_{A,ref}(\rho_w)}{\Delta\tau}\right]^{k_t(\rho_w)}. \tag{21}$$

Focussing attention now on VA situations, assume that the welded detail, in the as-welded condition, sketched in Fig. 3a is subjected to a system of external forces resulting, at the critical location, in a VA multiaxial stress state (Fig. 3b). As discussed in the previous section, under VA fatigue loading as well the orientation of the critical plane can directly be determined by locating that plane containing the direction, MV, experiencing the maximum variance of the resolved shear stress [30] (Fig. 3c). By using the appropriate definitions, the range of the shear, $\Delta\tau$, and normal, $\Delta\sigma_n$, stress relative to the critical plane can then be calculated directly (Fig. 3d and e), by subsequently determining the value of stress ratio ρ_w (Fig. 3f). As soon as ρ_w is known, by taking full advantage of Eqs (14) and (15) the position of the pertinent modified Wöhler curve has to be estimated by correcting the curve itself in order to properly take into account the damaging effect of those stress cycles of low stress amplitude (Fig. 3g). In more detail, according to Haibach [41], the negative inverse slope in the long-life regime has to be corrected as follows:

$$m_\tau(\rho_w) = 2 \cdot k_\tau(\rho_{w,lim}) - 1 \quad \text{for } \rho_w \leqslant 1 \tag{22}$$

$$m_\tau(\rho_w) \equiv 2 \cdot k - 1 = \text{const} \quad \text{for } \rho_w > 1 \tag{23}$$

where, for the same reason as above, also under VA fatigue loading the knee point is recommended to be always taken at $N_{kp} = 10^8$ cycles to failure.By taking full advantage of the classical Rain-Flow method [32], the resolved shear stress cycles can now be counted (Fig. 3h) to build the corresponding load spectrum (Fig. 3i) [31]. Finally, the calculated load spectrum can directly be used, along with the adopted modified Wöhler curve, to evaluate the damage content associated with any counted shear stress cycles (Fig. 3i and g), the estimated number of cycles to failure being equal to (Fig. 3k and l):

$$D_{tot} = \sum_{i=1}^{j} \frac{n_i}{N_{f,i}} \Rightarrow N_{f,e} = \frac{D_{cr}}{D_{tot}} \sum_{i=1}^{j} n_i. \tag{24}$$

In the above equations, D_{tot} is the total value of the damage sum, whereas D_{cr} is the critical value of the damage sum, i.e., the value of D_{tot} resulting in the fatigue breakage of the welded component being designed. Finally, it is worth observing that, as recommended by the IIW [3], the critical value of the damage sum, D_{cr}, is suggested as being taken invariably equal to 0.5.

To conclude, it has to be pointed out that, compared to our initial simplified proposals [28,42], the approach proposed in the present paper allows the VA problem to efficiently and accurately be addressed independently from the complexity of the assessed load history. On the contrary, since in Ref. [28,42] fatigue damage

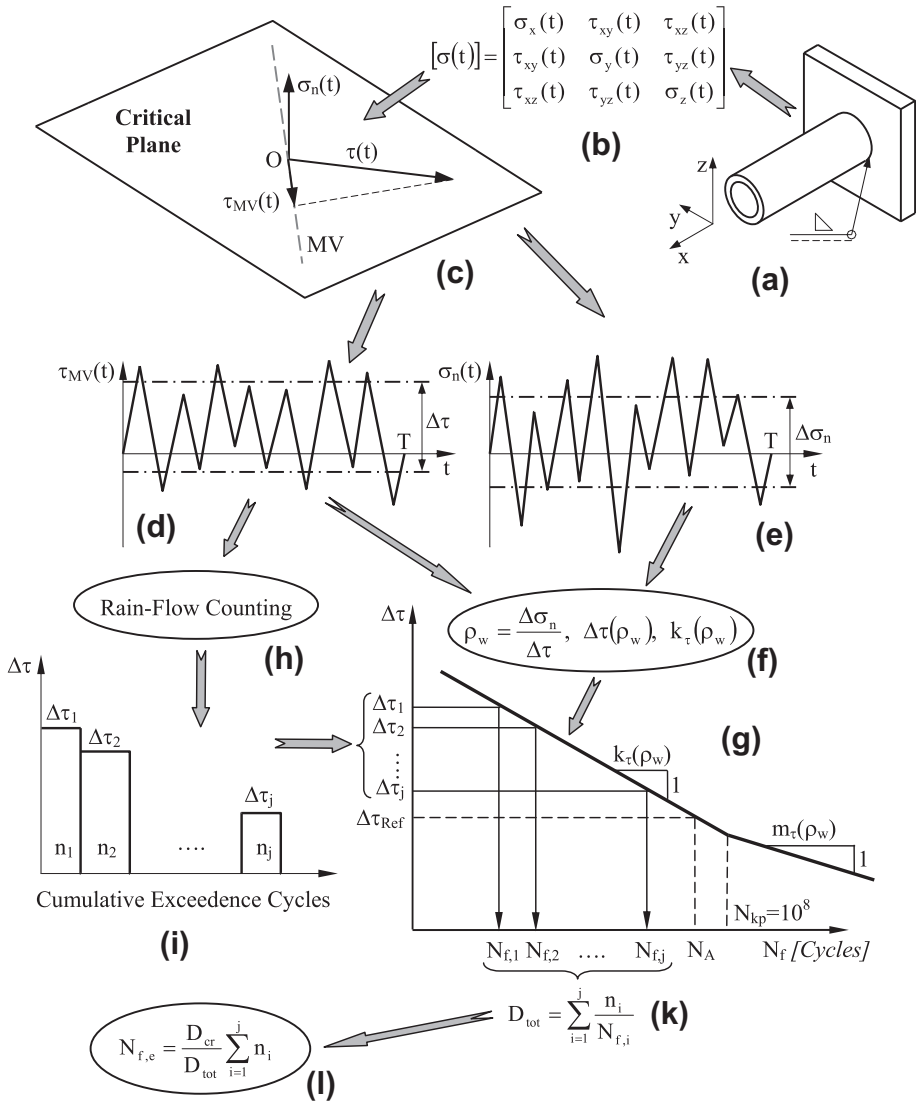

Fig. 3. Design against VA multiaxial fatigue loading.

was suggested as being estimated by following a cycle-by-cycle procedure, such a simplified method could unambiguously be applied solely to those situations involving VA multiaxial loading paths characterised by stress components having the same frequency.

4. Summary of the investigated data sets

In order to check the accuracy of the MWCM in estimating fatigue lifetime under multiaxial fatigue loading when our critical plane approach is applied in terms of either nominal stresses, hot-spot quantities, the reference radius concept, or the Theory of Critical Distances, a number of data sets were selected from the technical literature. In more detail, for comparison purposes, our approach was initially employed to estimate fatigue results generated under CA multiaxial fatigue loading. The selected CA series are listed in Table 1, whereas the investigated welded geometries are sketched in Fig. 4a–f. In order to concisely summarise the fatigue behaviour of the considered welded samples, Table 1 reports, for any investigated data sets, the uniaxial as well as the torsional fatigue curves, where such fatigue curves, estimated for a probability of survival, P_S, equal to 97.7%, are summarised in terms of negative inverse slope, k and k_0, reference nominal stress range, $\Delta\sigma_A$ and $\Delta\tau_A$, and scatter ratio of the stress amplitude, T_σ and T_τ, at $N_A = 2 \times 10^6$ cycles to failure for 90% and 10% probabilities of survival. With regard to the performed statistical reanalysis, the fatigue curves listed in Table 1 were calculated under the hypothesis of a log-normal distribution of the number of cycles to failure for each stress level and assuming a confidence level equal to 95% [43]. Finally, it is worth observing here also that, in light of their intrinsic VA nature [56], also the results generated both by Archer [50] and by Yousefi et al. [44] under CA bending and shear stress at different frequencies were considered in the present investigation. The main features of the results generated under VA multiaxial fatigue loading are instead summarised in Table 2, where $\Delta\Sigma_i$ and ΔT_i are the ranges of the uniaxial and torsional nominal stress during the loading cycles, respectively, δ is the out of phase angle and, finally, F is the ratio between the frequency of the axial stress component, f_Σ, and the frequency of the torsional stress component, f_T. It is important to highlight here that, for any data sets listed in Table 2, the corresponding uniaxial and torsional fatigue curves generated under CA fatigue loading are reported in Table 1.

To conclude, it has to be pointed out that all the fatigue results summarised in Table 2 were generated by adopting the classical

Table 1
Summary of the uniaxial and torsional experimental fatigue curves calculated in terms of nominal stresses.

Code	Material	Reference	t (mm)	z (mm)	R	k	$\Delta\sigma_A$ [b] (MPa)	T_σ	R	k_0	$\Delta\tau_A$ [b] (MPa)	T_τ	Geometry
WSP1	StE 460[a]	[14]	10	9	−1	4.4	152.0	1.703	−1	4.8	122.4	1.531	Fig. 4a
WSP2	StE 460[a]	[44]	8	10	−1, 0	3.9	125.7	1.759	−1	7.4	151.6	1.289	Fig. 4a
WSP3	StE 460	[45]	7.7	9	−1, 0	5.4	116.7	2.672	−1, 0	6.2	104.9	1.302	Fig. 4a
WSP4	A519	[46]	7.95	≈8	−1	5.4	90.7	1.528	−1	3.7	65.3	–	Fig. 4b
WSP5	A519 – A36[a]	[47]	9.525	8	−1, 0	3.8	123.9	1.324	−1, 0	5.5	103.9	1.613	Fig. 4b
WSP6	Fe 52 steel	[48,49]	5	6	0.1–0.7	2.2	46.7	7.511	−1, 0	3.5	85.2	3.852	Fig. 4c
WSP7	BS4360	[50]	6	≈10	0	–	–	–	−1	2.9	69.9	2.025	Fig. 4d
WSP8	BS4360 Gr. 50E	[51,52]	3.2	11	0	3.0	56.1	1.319	0	4.5	82.7	2.166	Fig. 4b
WSP9	42CrMo4[a]	[53]	5.5	n.a.	–	–	–	–	−1	14.6	167.6	1.243	Fig. 4f
WSP10	6082-T6	[54]	10	16	−1	6.8	60.3	1.845	−1	5.6	52.0	1.724	Fig. 4a
WSP11	6060-T6[a]	[55]	3	3	−1	5.4	68.3	1.222	–	–	–	–	Fig. 4e

[a] Stress relieved.
[b] Nominal reference stress ranges are calculated for $P_S = 97.7\%$ and extrapolated at $N_A = 2 \times 10^6$ cycles to failure.

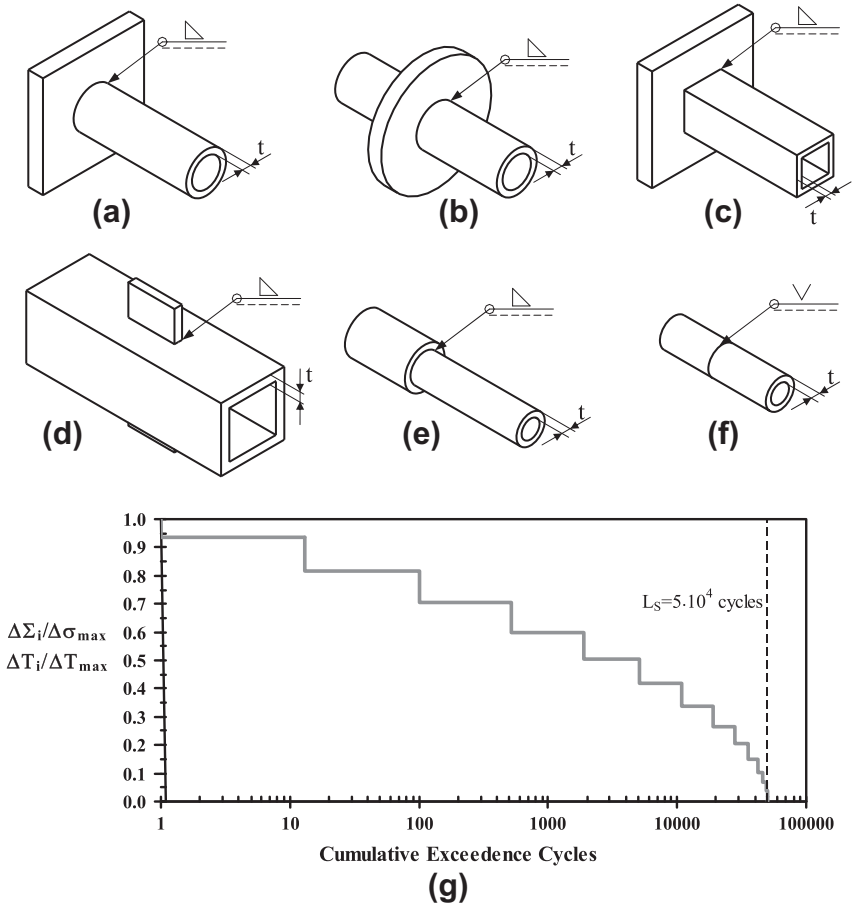

Fig. 4. Schematic geometry of the investigated welded samples (a–f) and LBS Gaussian Spectrum (g) [14].

LBF Gaussian spectrum sketched in Fig. 4g and having sequence length equal to 5×10^4 cycles [14].

5. Estimating lifetime in terms of nominal stresses

The most simple way of using the MWCM to perform the fatigue assessment of welded joints subjected to in-service CA and VA multiaxial fatigue loading is by calculating the relevant stress states at the assumed critical locations in terms of nominal stresses [24,33].

As soon as the nominal stress components damaging the welded detail being assessed are known, the MWCM can directly be applied as discussed in the previous Sections solely to perform the fatigue assessment of weldments working in the as-welded condition. On the contrary, to reduce the estimates' level of conservatism, stress relieved welded joints are recommended to be designed against fatigue by multiplying the reference shear stress range of the adopted modified Wöhler curve by a suitable enhancement factor, $f(R_{CP})$, that is [3]:

$$\Delta\tau_{Ref}(\rho_w)\cdot f(R_{CP}) = (a\cdot\rho_w + b)\cdot f(R_{CP}) \tag{25}$$

where factor $f(R_{CP})$ is assumed [40] to depend on the load ratio, R_{CP}, calculated through the stress perpendicular to the critical plane, i.e. [39]:

$$R_{CP} = \frac{\sigma_{n,m} - \sigma_{n,a}}{\sigma_{n,m} + \sigma_{n,a}} \tag{26}$$

Table 2
Summary of the fatigue results generated under VA fatigue loading.

Code	Material	Reference	R	$\Delta\Sigma_i/\Delta T_i$	δ (°)	F	Geometry	Spectrum
WSP1	StE 460[a]	[14]	−1	∞	–	–	Fig. 4a	Fig. 4g
			−1	0	–	–		
			−1	$\sqrt{3}$	0	1		
			−1	$\sqrt{3}$	90	1		
WSP2	StE 460[a]	[44]	−1	∞	–	–	Fig. 4a	Fig. 4g
			−1	1	0	1		
			−1	1	90	1		
			−1	1	0	5		
			0	1	0	1		
			0	1	90	1		
WSP9	42CrMo4	[53]	−1	0	–	–	Fig. 4f	Fig. 4g
WSP10	6082-T6	[22]	−1	∞	–	–	Fig. 4a	Fig. 4g
			−1	$\sqrt{3}$	0	1		
			−1	$\sqrt{3}$	90	1		

[a] Stress relieved.

$\sigma_{n,a}$ and $\sigma_{n,m}$ being the amplitude and the mean value of normal stress $\sigma_n(t)$, respectively (obviously both stress quantities have to be determined according to either the CA or the VA definitions reviewed above). The idea of using solely the stress perpendicular to the critical plane to estimate in stress relieved welded joints the damaging effect of superimposed static stresses is based on the experimental evidence that in non-welded metallic materials the presence of non-zero mean shear stresses can be neglected as long as the maximum shear stress (during the loading cycle) is lower than the material yield shear stress [57,58]. Therefore, according the above considerations, the rules recommended in Ref. [34] can directly be extended to CA and VA multiaxial fatigue situations as follows [40]:

$$\begin{aligned} f(R_{CP}) &= 1.32 \text{ for } R_{CP} < -1 \\ f(R_{CP}) &= -0.22 \times R_{CP} + 1.1 \text{ for } -1 \leqslant R_{CP} \leqslant 0 \\ f(R_{CP}) &= -0.2 \times R_{CP} + 1.1 \text{ for } 0 < R_{CP} \leqslant 0.5 \\ f(R_{CP}) &= 1 \text{ for } R_{CP} > 0.5 \end{aligned} \quad (27)$$

for steel welded joints and

$$\begin{aligned} f(R_{CP}) &= 1.88 \text{ for } R_{CP} < -1 \\ f(R_{CP}) &= -0.55 \times R_{CP} + 1.33 \text{ for } -1 \leqslant R_{CP} \leqslant 0 \\ f(R_{CP}) &= -0.66 \times R_{CP} + 1.33 \text{ for } 0 < R_{CP} \leqslant 0.5 \\ f(R_{CP}) &= 1 \text{ for } R_{CP} > 0.5 \end{aligned} \quad (28)$$

for aluminium welded joints.

The experimental, N_f, vs. estimated, $N_{f,e}$, fatigue lifetime diagrams reported in Fig. 5 summarise the overall accuracy of the MWCM, applied in terms of nominal stresses, in estimating fatigue strength of both as-welded and stress relived joints subjected to CA as well as to VA fatigue loading, the adopted axial and torsional calibration fatigue curves (see Table 3) being those recommended by the IIW [3]. With regard to these error diagrams, it is worth observing here also that the plotted scatter bands were recalculated from the reference value of 1.5 suggested by Haibach and determined by considering fatigue curves characterised by a probability of survival equal to 10% and 90%, respectively [59]: consistently, the scatter ratio of the stress range at 2×10^6 cycles to failure for 97.7% and 2.3% probabilities of survival is equal to 1.85. Further, both the uniaxial and torsional scatter bands were shifted parallel to the abscissa by forcing the straight lines characterised by a probability of survival equal to 2.3% to coincide with the $N_f = N_{f,e}$ straight diagonal line. The error diagrams of Fig. 5 clearly prove that the MWCM applied in terms of nominal stresses is highly accurate in estimating fatigue lifetime of welded joints subjected to both CA (Fig. 5a and b) and VA in-service fatigue loading (Fig. 5c), resulting in estimates falling within the two scatter bands associated with the uniaxial and torsional standard fatigue curves used to calibrate the MWCM itself. This means that the MWCM applied in terms of nominal stresses is capable of performing the fatigue assessment under both CA and VA fatigue loading by complying with the recommendations of the available standard codes, that is, by always resulting in estimates characterised, from a statistical point of view, by an adequate level of safety. As to the estimates obtained for those welded samples tested under VA fatigue loading (Fig. 5c), according to what recommended by the IIW [3], fatigue lifetime was predicted by taking the critical value of the damage sum, D_{cr}, invariably equal to 0.5. Further, the estimates summarised in the chart of Fig. 5c were calculated adopting the classical "2k−1 correction" due to Haibach [41], Eqs (22) and (23), with $N_{kp} = 10^8$ cycles to failure.

To conclude, it can be pointed out that the reached level of accuracy is definitely satisfactory because one cannot ask a predictive method to result in estimates that are, from a statistical point of view, less scattered than the experimental information used to calibrate the method itself.

6. Estimating lifetime in terms of hot-spot stresses

In order to correctly apply the MWCM in terms of hot-spot stresses to estimate multiaxial fatigue lifetime of weldments, the stress components relative to the critical plane are suggested as being determined by post-processing the geometrical stress components perpendicular (σ_{HS} in Fig. 6a) and parallel (τ_{HS} in Fig. 6a) to the weld bead [60]. In particular, such stress components are recommended to be used to define the relevant stress state at the assumed critical section because in the presence of notches with opening angle larger than about 100°, fatigue strength is seen to depend mainly on the Mode I and III stress components [16]. On the contrary, the contribution of Mode II loading to the overall fatigue damage can be neglected with little loss of accuracy as a consequence of the fact that the resulting stress components are not singular [6]. According to the above considerations and owing to the fact that the magnitude of the geometrical stresses is seen to vary as the distribution of the linear-elastic stress fields in the vicinity of the hot-spots changes [61], it is possible to hypothesise that the structural stresses perpendicular to the weld bead are somehow related to the Mode I stress components, whereas the

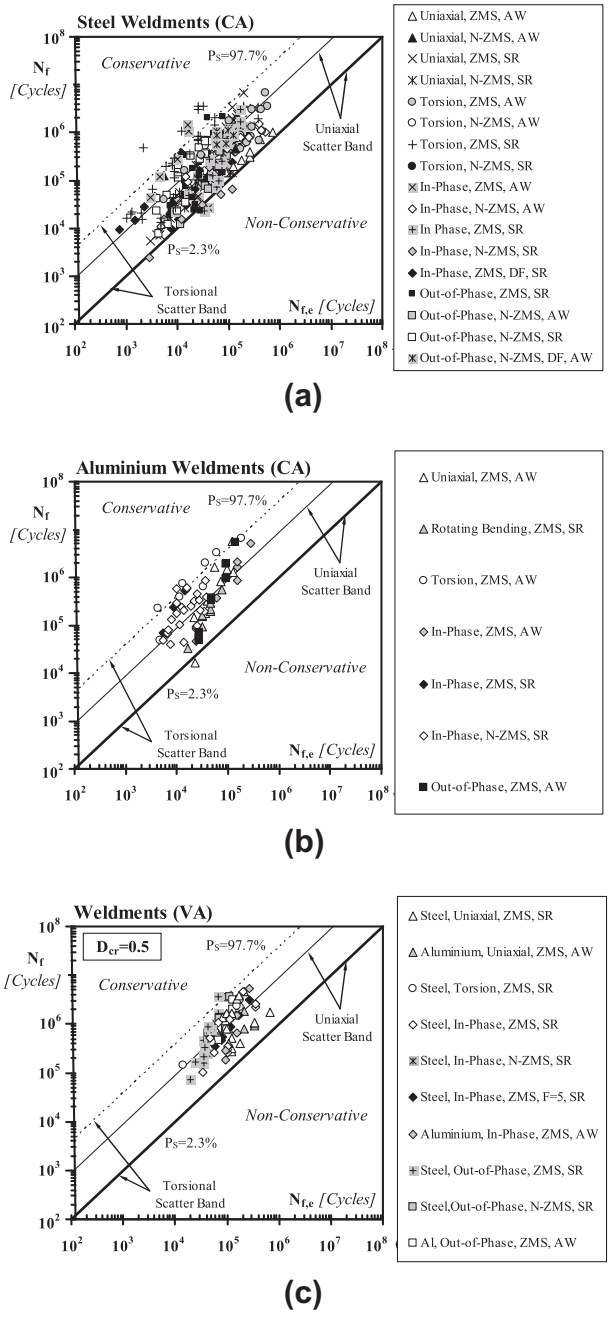

Fig. 5. Accuracy of the MWCM applied in terms of nominal stresses in estimating fatigue lifetime of steel and aluminium weldments subjected to CA (a and b) and VA (c) uniaxial/multiaxial fatigue loading (ZMS = zero mean stress; N-ZMS = non-zero mean stress; AW = as-welded; SR = stress relieved; DF = different frequencies; $F = f_{\Sigma}/f_T$).

structural shear stresses parallel to the weld bead depend instead on the Mode III stress components [24,60].

As to the performed validation exercise, Fig. 6a schematically shows the strategy we followed to calculate the hot-spot stress states in the investigated welded geometries (Fig. 4a–f). In more detail, normal and shear structural stresses were extrapolated to the weld toe by using two superficial points positioned at a distance from the hot-spot equal to $0.4t$ and t, respectively [3], t being the reference thickness as defined in Fig. 4a–f. The stress values used to extrapolate the hot-spot quantities were determined at the above reference points through linear-elastic FE models whose mesh density was set according to Niemi's recommendations [5].

With regard to the in-field usage of the MWCM applied in terms of hot-spot quantities to perform the fatigue assessment of stress relived welded joints, superimposed static stresses were taken into account by directly correcting the modified Wöhler curves through enhancement factor $f(R_{CP})$, Eq. (25), where the above factor was calculated again according to definitions (27) and (28).

The experimental, N_f, vs. estimated, $N_{f,e}$, number of cycles to failure diagrams reported in Fig. 6b–d were built by calibrating the constants in the MWCM's governing equations through the reference values suggested by the IIW [3] and summarised in Table 4. The above error diagrams should make it evident that the use of the MWCM applied in terms of hot-spot stresses results in estimates falling, mainly on the conservative side, within the widest calibration scatter band.

To conclude, it can be highlighted that also in this case fatigue lifetime under VA fatigue loading (Fig. 6d) was estimated by taking the critical value of the damage sum, D_{cr}, constant and equal to 0.5 [3] as well as by adopting, as recommended by Haibach [41], the classical "2k−1 correction", Eqs (22) and (23), with $N_{kp} = 10^8$ cycles to failure.

7. Estimating lifetime according to the reference radius concept

The most advanced design methodology which is recommended by the IIW [3] is that based on the use of a reference radius, r_{ref}, equal to 1 mm, where such a method can be adopted solely to perform the fatigue assessment of welded joints having thickness of the main plate larger than (or equal to) 5 mm. In more detail, according to the above approach the profile of either the weld toe or root is rounded with a circular fillet having radius equal to 1 mm (Fig. 7a). From a scientific point of view, the above value for r_{ref} was first proposed by Radaj [4,62] who took full advantage of the micro-support theory due to Neuber to model the fatigue behaviour of sharp cracks: accordingly, the fatigue assessment performed in terms of the reference radius concept is seen not to be influenced by the actual values of the radii of either the weld toes or roots [62].

If lifetime under uniaxial fatigue loading is estimated according to such a well-established method, the IIW suggests using a reference stress range, $\Delta\sigma_A$, calculated, according to the maximum principal stress criterion at $N_A = 2\times10^6$ cycles to failure, equal to 225 MPa for steel weldments and to 71 MPa for aluminium joints, the above reference ranges being determined for a probability of survival, P_S, equal to 97.7% and estimated under a load ratio, R, equal to 0.5 (i.e., by simulating the effect of high tensile residual stresses). Further the CA uniaxial fatigue curve recommended by the IIW has the knee point, N_{kp}, at 10^7 cycles to failure and negative inverse slope k is equal to 3 for $N_f \leqslant N_{kp}$ and to 22 for $N_f > N_{kp}$ [4,34], this schematisation applying to both steel and aluminium weldments.

Under CA torsional loading instead, the design curve, again determined according to the maximum principal stress hypothesis, suggested by Sonsino [34] as being used to perform the fatigue assessment according to the $r_{ref} = 1$ mm idea has reference shear stress range, $\Delta\tau_A$, at $N_A = 2\cdot10^6$ cycles to failure equal to 160 MPa and to 63 MPa for steel and aluminium welded joints, respectively. Further, the negative inverse slope, k_0, is equal to 5 for $N_f \leqslant N_{kp}$ and to 22 for $N_f > N_{kp}$, where N_{kp} is taken equal to 10^8 cycles to failure.

Strictly speaking, the curves as defined above can safely be used to design against fatigue solely those as-welded structures that can be classified as "thick and stiff". On the contrary, as long as "thin and flexible" welded structures are concerned, the negative inverse slope is seen to increase from 3 up to 5 under CA uniaxial fatigue loading and from 5 up to 7 under CA torsional loading [63]. As to the above schematisation, it has to be said that, even though in

Table 3
Fatigue curves used to calibrate the MWCM to apply it in terms of nominal stresses.

Code	Material	Reference	k	$\Delta\sigma_A$[b] (MPa)	k_0	$\Delta\tau_A$[b] (MPa)	Geometry
WSP1	StE 460[a]	[14]	3	71	5	100	Fig. 4a
WSP2	StE 460[a]	[44]	3	71	5	100	Fig. 4a
WSP3	StE 460	[45]	3	71	5	100	Fig. 4a
WSP4	A519	[46]	3	71	5	80	Fig. 4b
WSP5	A519 – A36[a]	[47]	3	71	5	100	Fig. 4b
WSP6	Fe 52 steel	[48,49]	3	45	5	100	Fig. 4c
WSP7	BS4360	[50]	3	80	5	80	Fig. 4d
WSP8	BS4360 Gr. 50E	[51,52]	3	71	5	80	Fig. 4b
WSP9	42CrMo4[a]	[53]	–	–	5	100	Fig. 4f
WSP10	6082-T6	[54]	3	32	5	36	Fig. 4a
WSP11	6060-T6[a]	[55]	3	22	5	28	Fig. 4e

[a] Stress relieved.
[b] Nominal reference stress ranges (P_S = 97.7%) extrapolated at $N_A = 2 \times 10^6$ cycles to failure.

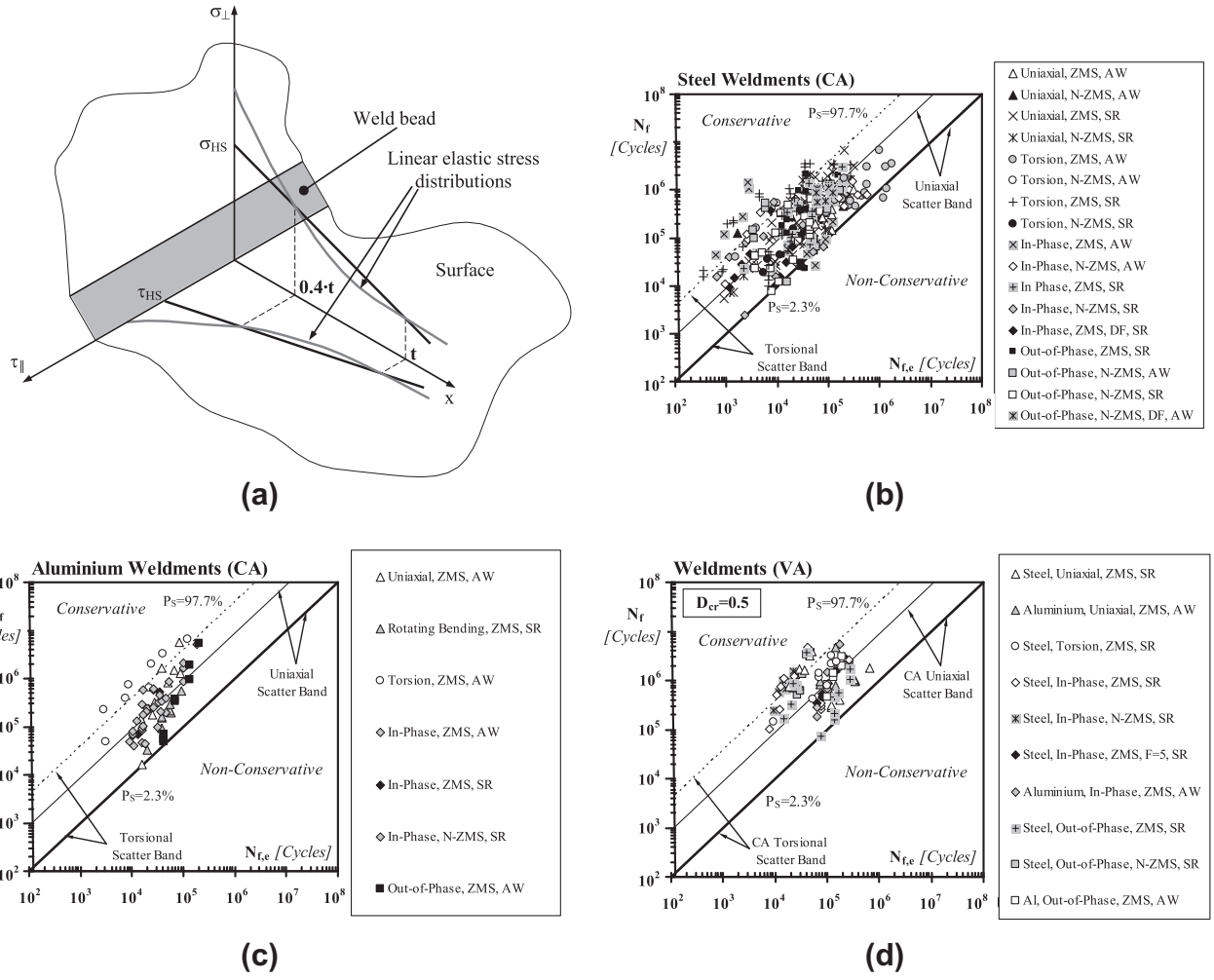

Fig. 6. Accuracy of the MWCM applied in terms of hot-spot stresses in estimating fatigue lifetime of steel and aluminium weldments subjected to CA (b and c) and VA (d) uniaxial/multiaxial fatigue loading (ZMS = zero mean stress; N-ZMS = non-zero mean stress; AW = as-welded; SR = stress relieved; DF = different frequencies; $F = f_\Sigma/f_T$).

situations of practical interest it is never straightforward to classify welded joints as either "thick and stiff" or "thin and flexible", in the validation exercise discussed below the use of the r_{ref} = 1 mm idea will be extended to those situations involving both CA and VA multiaxial fatigue loading by taking into account also this important aspect: according to the above considerations, Table 5 summarises the fatigue curves used to calibrate the constants in the MWCM's governing equations to make our criterion suitable for being applied, in conjunction with the r_{ref} = 1 mm approach [40], to the investigated experimental results.

Another important aspect which has to be considered in great detail here is the problem of correctly locating the point at which the critical stress has to be calculated in order to accurately perform the fatigue assessment according to the reference radius idea (point O in Fig. 7a). In particular, it has to be highlighted that, in the most general case, the peak of the stress state may be positioned,

Table 4
Fatigue curves used to calibrate the MWCM to apply it in terms of hot-spot stresses.

Code	Material	Reference	k	$\Delta\sigma_A$[b] (MPa)	k_0	$\Delta\tau_A$[b] (MPa)	Geometry
WSP1	StE 460[a]	[14]	3	90	5	100	Fig. 4a
WSP2	StE 460[a]	[44]	3	90	5	100	Fig. 4a
WSP3	StE 460	[45]	3	90	5	100	Fig. 4a
WSP4	A519	[46]	3	90	5	100	Fig. 4b
WSP5	A519 – A36[a]	[47]	3	90	5	100	Fig. 4b
WSP6	Fe 52 steel	[48,49]	3	90	5	100	Fig. 4c
WSP7	BS4360	[50]	3	90	5	100	Fig. 4d
WSP8	BS4360 Gr. 50E	[51,52]	3	90	5	100	Fig. 4b
WSP9	42CrMo4[a]	[53]	–	–	5	100	Fig. 4f
WSP10	6082-T6	[54]	3	36	5	36	Fig. 4a
WSP11	6060-T6[a]	[55]	3	36	5	36	Fig. 4e

[a] Stress relieved.
[b] Hot-spot reference stress ranges (P_S = 97.7%) extrapolated at $N_A = 2 \times 10^6$ cycles to failure.

along the fictitious fillet, at different points as the degree of multiaxiality and non-proportionality of the applied load history varies. However, in practise the above difference is seen to be so small to be negligible; if not, it is evident that the correct position of the critical location has to be found by looking for that point experiencing the largest extent of fatigue damage [40].

The uniaxial and torsional reference curves as defined above can efficiently be used to calibrate the constants in the MWCM's governing equations to use our criterion solely to design welded joints working in the as-welded condition. On the contrary, in order to correctly take into account the mean stress effect in stress relieved welded connections, the stress range at N_A cycles to failure of any modified Wöhler curve can directly be corrected through enhancement factor $f(R_{CP})$, Eq. (25), such a factor being again calculated according to definitions (27) and (28) [34].

The charts reported in Fig. 7b–d show the accuracy of the MWCM, used in conjunction with the reference radius concept, in estimating CA fatigue lifetime of "thin and flexible" as well as "thick and stiff" welded joints of both steel (Figs. 7b and c) and aluminium (Fig. 7d). As to the above diagrams, it is worth observing that the reference scatter bands are wider for "thin and flexible" joints due to the fact that in such circumstances the negative inverse slope is equal to 5 under uniaxial loading and to 7 under torsion [63]. Further, in the above charts the results generated by both Razmijoo [51,52] and Costa et al. [55] were not considered, because in those samples the thickness of the main tube was lower than 5 mm. The accuracy of the MWCM in estimating lifetime under VA fatigue loading is instead summarised in the error diagrams of Fig. 7e, the above predictions being made according to the "2k−1 correction" proposed by Haibach [41], Eqs (22) and (23), with $N_{kp} = 10^8$ cycles to failure.

As to the above error diagrams, it is worth observing that the obtained estimates are characterised not only by an higher scattering level, but also by an higher level of conservatism. This evidence can be ascribed to the fact that the scientific research community has not agreed yet a unique reference curve suitable for performing, according to the reference radius concept, the fatigue assessment of welded joints loaded in torsion [34]. This implies that when the curves recommended by Sonsino [34] is adopted, the lifetime predicted under torsional fatigue loading is sometimes characterised by an excessive level of conservatism [40]. Accordingly, since the constants in the MWCM's governing equations are calibrated not only through the uniaxial, but also through the torsional reference design curves, the systematic usage of our approach to estimate fatigue lifetime under both CA and VA multiaxial fatigue loading resulted in estimates that are characterised by a higher level of both scattering and conservatism. The above considerations suggests that more experimental work needs to be done in order to propose reference fatigue curves allowing fatigue lifetime under torsional loading to be estimated more accurately.

To conclude, it is possible to say that, in spite of the above limitations, the MWCM is seen to be successful in performing the fatigue assessment under both CA and VA fatigue loading also when it is applied in terms of the r_{ref} = 1 mm approach: as shown in the error diagrams reported in Fig. 7b-e, the obtained estimates not only fall mainly within the calibration scatter bands, but they are also characterised by a level of conservatism that definitely complies with the recommendations of the available standard codes.

8. Estimating lifetime according to the Theory of Critical Distances

It is the author's opinion that, even if its accuracy and reliability is not brought into question at all, the real difficulty in using the reference radius idea to design welded joints against fatigue in situations of practical interest is that determining the necessary stress states by rounding weld beads and roots with a fictitious radius is a complex and time-consuming numerical job, this holding true especially when complex tridimensional geometries are involved. In order to overcome the above problem without missing the advantages of linear-elastic local analyses, we have recently devised a novel design method which is based on the use of the MWCM applied along with the Theory of Critical Distances (TCD), the latter being formalised in terms of the so-called Point Method (PM) [10,11,24]. In more detail, such an approach can be used to estimate fatigue damage in welded connections by directly post processing the linear-elastic stress fields damaging the material in the vicinity of the assumed crack initiation sites, weld beads and roots being simply modelled as sharp notches. The most relevant peculiarity of our method is that, thanks to its specific features, it allows welded components to be assessed by simultaneously taking into account not only the degree of multiaxiality and non-proportionality of the linear-elastic stress field acting on the process zone, but also the detrimental effect of time-variable multiaxial stress gradients [64,65].

The in-field procedure suggested as being followed to perform the stress analysis according to our local approach is shown in Fig. 8. In particular, consider a welded joint damaged by a complex system of cyclic forces: as schematically displayed in Fig. 8, the stress state to be used to determine the necessary stress quantities relative the critical plane has to be determined, along the bisector, at a distance from the weld toe apex (or the weld root apex) equal to M-D_V, such a critical distance being equal to 0.5 mm and to 0.075 mm for steel and aluminium welded joints, respectively [64,65]. Further, it is worth pointing out here also that, according to the TCD's philosophy, critical length M-D_V is assumed to be a material property whose value does not depend on either the

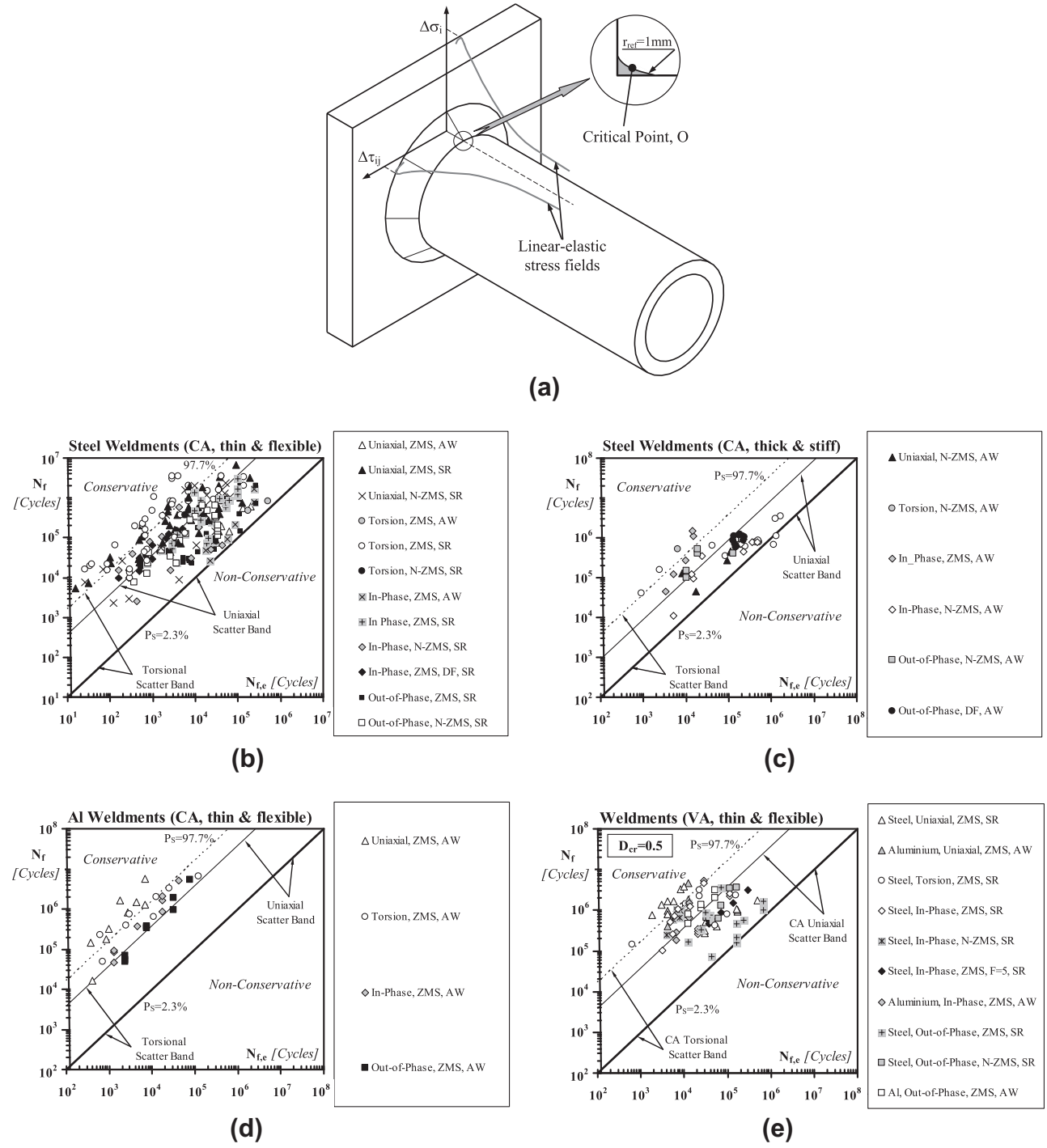

Fig. 7. Accuracy of the MWCM applied along with the reference radius concept in estimating fatigue lifetime of steel and aluminium weldments subjected to CA (b–d) and VA (e) uniaxial/multiaxial fatigue loading (ZMS = zero mean stress; N-ZMS = non-zero mean stress; AW = as-welded; SR = stress relieved; DF = different frequencies; $F = f_{\Sigma}/f_T$).

geometrical feature of the welded detail being assessed or the complexity of the stress field acting on the process zone [24].

As soon as the time-variable stress state at the critical point is known, the range of the maximum shear stress, $\Delta\tau$, and the range of the stress perpendicular to the critical plane, $\Delta\sigma_n$, can directly be determine by taking full advantage of either the CA or the VA definitions reviewed above. Finally, the calculated value for ratio ρ_w allows the negative inverse slope, $k_\tau(\rho_w)$, and the reference shear stress range, $\Delta\tau_{Ref}(\rho_w)$, of the appropriate modified Wöhler curve to be estimated from the calibration functions reported below. In particular, for steel welded joints the negative inverse slope is suggested as being calculated as [64]:

$$k_\tau(\rho_w) = -2 \cdot \rho_w + 5 \quad \text{for } \rho_w \leqslant 1 \tag{29}$$

$$k_\tau(\rho_w) = 3 \quad \text{for } \rho_w > 1 \tag{30}$$

whereas the reference shear stress ranges, $\Delta\tau_{Ref}(\rho_w)$, at $N_A = 5 \times 10^6$ cycles to failure takes on the following values [64]:

$$\Delta\tau_{Ref}(\rho_w) = -32 \cdot \rho_w + 96 \text{ [MPa]} \quad \text{for } \rho_w \leqslant 2 \tag{31}$$

Table 5
Fatigue curves used to calibrate the MWCM to apply it along with the r_{ref} = 1 mm concept.

Code	Material	Reference	k	$\Delta\sigma_A$[b] (MPa)	k_0	$\Delta\tau_A$[b] (MPa)	$\rho_{w,lim}$	Geometry
WSP1	StE 460[a]	[14]	5	225	7	160	1.7	Fig. 4a
WSP2	StE 460[a]	[44]	5	225	7	160	1.7	Fig. 4a
WSP3	StE 460	[45]	5	225	7	160	1.7	Fig. 4a
WSP4	A519	[46]	5	225	7	160	1.7	Fig. 4b
WSP5	A519 – A36[a]	[47]	5	225	7	160	1.7	Fig. 4b
WSP6	Fe 52 steel	[48,49]	3	225	5	160	1.7	Fig. 4c
WSP7	BS4360	[50]	3	225	5	160	1.7	Fig. 4d
WSP9	42CrMo4[a]	[53]	–	–	7	160	1.45	Fig. 4f
WSP10	6082-T6	[54]	5	71	7	63	1.45	Fig. 4a

[a] Stress relieved.
[b] Local reference stress ranges (P_S = 97.7%) extrapolated at $N_A = 2 \times 10^6$ cycles to failure.

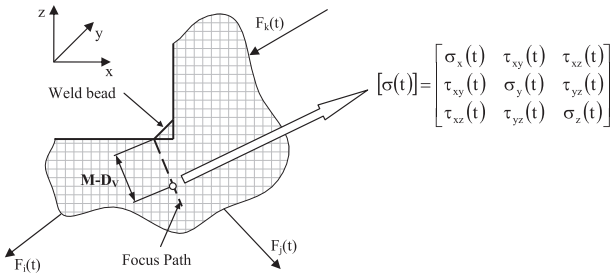

Fig. 8. Definition of the focus path and stress state at distance M-D_V.

$$\Delta\tau_{Ref}(\rho_w) = 32 \text{ [MPa]} \quad \text{for } \rho_w > 2 \tag{32}$$

for a probability of survival, P_S, equal to 50%, and [42]:

$$\Delta\tau_{A,Ref}(\rho_w) = -24 \cdot \rho_w + 67 \text{ [MPa]} \quad \text{for } \rho_w \leqslant 2 \tag{33}$$

$$\Delta\tau_{A,Ref}(\rho_w) = 19 \text{ [MPa]} \quad \text{for } \rho_w > 2 \tag{34}$$

for P_S = 97.7%.

For aluminium weldments the constants in the MWCM's governing equations are instead as follows, N_A being again equal to 5×10^6 cycles to failure [65]:

$$k_\tau(\rho_w) = -0.5 \cdot \rho_w + 5 \quad \text{for } \rho_w \leqslant 4 \tag{35}$$

$$k_\tau(\rho_w) = 3 \quad \text{for } \rho_w > 4 \tag{36}$$

$$\Delta\tau_{Ref}(\rho_w) = -1.3 \cdot \rho_w + 33.6 \text{ [MPa]} \quad \text{for } \rho_w \leqslant 4 \tag{37}$$

$$\Delta\tau_{Ref}(\rho_w) = 28.4 \text{ [MPa]} \quad \text{for } \rho_w > 4 \tag{38}$$

for P_S = 50%, and

$$\Delta\tau_{Ref}(\rho_w) = -5 \cdot \rho_w + 28 \text{ [MPa]} \quad \text{for } \rho_w \leqslant 4 \tag{39}$$

$$\Delta\tau_{Ref}(\rho_w) = 8 \text{ [MPa]} \quad \text{for } \rho_w > 4 \tag{40}$$

for a probability of survival, P_S, equal to 97.7%.

According to Eurocode 3 [1], Eurocode 9 [2] and the IIW recommendations [3], the $\Delta\tau_{Ref}$ vs. ρ_w relationships reported above are strictly valid solely to assess welded joints working in the as-welded condition [64,65]. On the contrary, if the welded joint being designed is stress relieved, then a procedure similar to the one recommended by Eurocode 3 [1] is proposed to be used [64]: an effective shear stress range can directly be determined by adding the tensile part to 60% of the compressive portion of the shear stress range. Accordingly, by adopting a strategy similar to the one recommended by the IIW [3], a suitable shear stress enhancement factor, $f(\tau)$, can directly be calculated as follows:

$$f(\tau) = 1 \quad \text{for } (\tau_m - \tau_a) \geqslant 0 \tag{41}$$

$$f(\tau) = \frac{2\tau_a}{|\tau_m + \tau_a| + 0.6|\tau_m - \tau_a|} \quad \text{for } (\tau_m - \tau_a) < 0 \tag{42}$$

As to the above correction, it is worth observing here that it can safely be used to design stress relieved welded joints made not only of steel (as recommended by Eurocode 3), but also of aluminium, since in the latter case the use of enhancement factor $f(\tau)$ results in corrections that are, in any case, more conservative than the ones obtained by adopting the enhancement factor values suggested by Sonsino as being used to specifically design stress relieved welded joints of aluminium [34].

Turning back to the determination of the stress state at the critical point (Fig. 8), it is worth highlighting here that, according to the TCD's philosophy, such a stress tensor has to be determined by using a linear-elastic constitutive law to model the behaviour of both the parent and welded material. It is evident that the above hypothesis results in a great simplification of the design problem, since the total stress state at any instant of the load history can be determined by superposing the effect of every applied force, whose contributions being computed separately. Further, the stress state at a distance from the assumed crack initiation point equal to M-D_V is recommended to be determined by always considering the contribution of the three fundamental modes (i.e., Mode I, II and III stress components) [24,64,65], even though, strictly speaking, fatigue damage in conventional welded joints can efficiently be evaluated by taking into account solely the contributions due to the singular modes (i.e., Mode I and III loading), Mode II stress components being no longer singular in the presence of stress raiser opening angles larger than about 100° [6]. This *modus operandi* results in an evident simplification of the stress analysis problem because, by so doing, our design methodology can be applied by directly post-processing the results calculated through simple linear-elastic FE models without the need for distinguishing *a priori* between singular and non-singular contributions.

In order to show the overall accuracy of our local approach, initially the error diagrams of Fig. 9a and b report the predictions made by considering a variety of steel welded details subjected to both CA (Fig. 9a) and VA (Fig. 9b) uniaxial nominal loading, the considered geometries as well as the investigated CA and VA loading paths being summarised, together with the corresponding bibliographical sources, in Refs [42,64]. The above charts should make it evident that our local method is capable of correctly evaluating the degree of multiaxiality of the stress field acting on the fatigue process zone, whose profile depends, in such circumstances, solely on the specific geometrical features of the assessed welded geometry. A similar level of accuracy is obtained also when the MWCM is used, along with the PM, to estimate the experimental results generated by testing steel weldments and summarised in Tables 1 and 2 (Fig. 9c and d), that is, when the degree of multiaxiality and non-proportionality of the local stress field depends not only on the geometrical features of the assessed welded

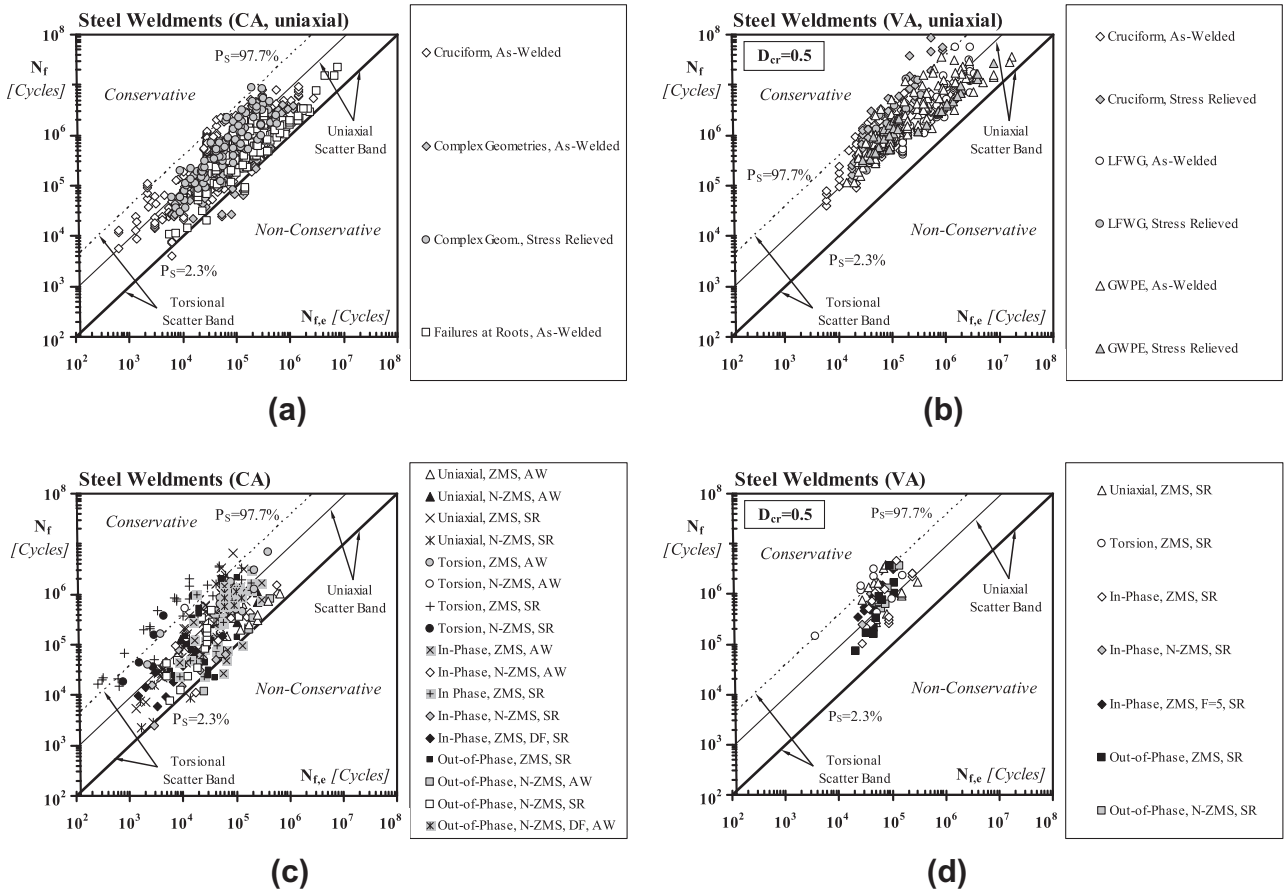

Fig. 9. Accuracy of the MWCM applied along with the Theory of Critical Distances in estimating fatigue lifetime of steel and aluminium weldments subjected to CA (a and c) and VA (b and d) uniaxial/multiaxial fatigue loading (LFWG = Longitudinal fillet welded gusset; GWPE = Gussets Welded on Plate Edges; ZMS = zero mean stress; N-ZMS = non-zero mean stress; AW = as-welded; SR = stress relieved; DF = different frequencies; $F = f_{\Sigma}/f_T$).

connection, but also on the specific characteristics of the investigated CA (Fig. 9c) and VA (Fig. 9b) load history.

The chart of Fig. 10a summarises instead the accuracy and reliability of our local method in estimating fatigue lifetime of aluminium welded joints subjected to CA uniaxial nominal loading, the geometries of the considered welded samples being described in great detail in Ref. [65]. The above chart suggests that as long as joints in the as-welded condition are concerned, the use of our method results in predictions falling mainly within the calibration scatter bands. On the contrary the estimates associated with stress relieved welded joints are, as expected, slightly conservative. A similar level of conservatism was obtained also when our approach was used to estimate the experimental data summarised in Tables 1 and 2 and generated by testing, under both CA (Fig. 10b) and VA (Fig. 10c) fatigue loading, welded samples of aluminium [22].

It is worth pointing out here that that also in this case the number of cycles of failure under VA fatigue loading (Figs. 9b, d and 10c) was predicted not only by taking $D_{cr} = 0.5$ [3], but also as by adopting the classical "2k−1 correction", Eqs (22) and (23), with $N_{kp} = 10^8$ cycles to failure.

Turning back to aluminium weldments, to understand the choice of suggesting the use of calibration constants which result in estimates characterised, from a statistical point of view, by an evident conservative trend, it is worth observing here that, according to the state of the art, the resources which have been invested so far to understand the response of aluminium welded joints to fatigue loadings are definitely very little compared to those invested to investigate the fatigue behaviour of welded steel. Such a lack of knowledge becomes absolutely evident when the available standard codes and recommendations are compared to each other: for instance, the fatigue design curves supplied by Eurocode 9 [2] are different from those recommended by the IIW [3] not only in terms of reference strength at 2 million cycles to failure, but also in terms of negative inverse slope [66]. The urgency of developing an efficient strategy to design aluminium weldments against multiaxial fatigue is proven by the fact that, as far as the writer is aware, only a few papers addressing the above problem and reporting original experimental results have been published in International Scientific Journals so far. Moreover, only one series of tests carried out under non-proportional loading is available in the technical literature. Finally, examination of the state of the art shows that, surprisingly, only few attempts have been made so far to devise reliable methodologies capable of efficiently estimating lifetime when aluminium weldments are subjected to variable amplitude multiaxial fatigue loading.

Another open question which should be answered urgently is the way of efficiently taking into account the presence of non-zero mean stresses, this holding true not only in stress relieved but also in as-welded joints: in fact, contrary to what happens in steel welded details, aluminium weldments can be highly sensitive to the presence of superimposed static stresses also when they work in the as-welded condition [67].

The above considerations should make it clear that, in light of such a level of uncertainty, as formalising our approach [24,65] we decided to calibrate the MWCM's governing equations through uniaxial and torsional reference curves allowing an adequate

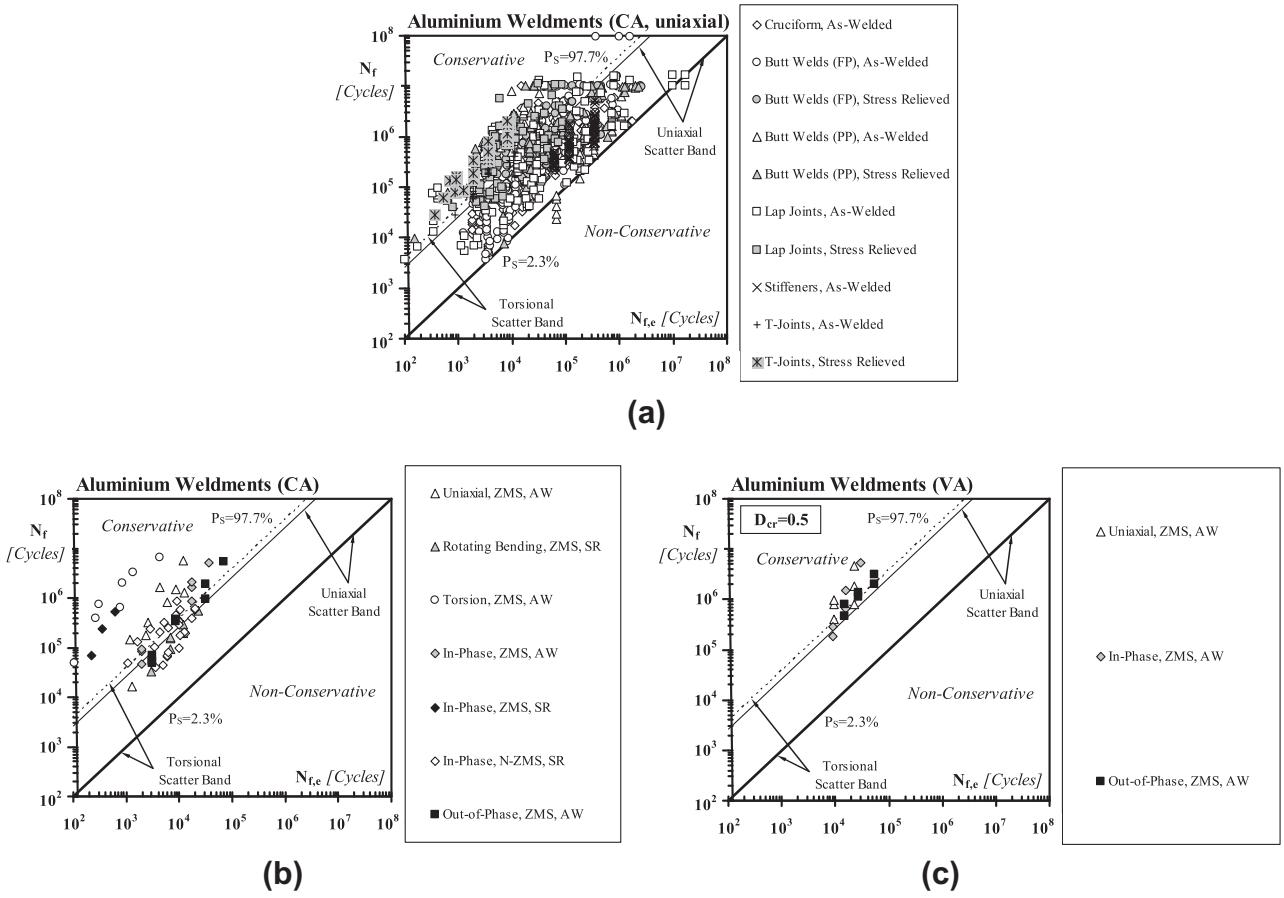

Fig. 10. Accuracy of the MWCM applied along with the Theory of Critical Distances in estimating fatigue lifetime of aluminium weldments subjected to CA (a and b) and VA (c) uniaxial/multiaxial fatigue loading (ZMS = zero mean stress; N-ZMS = non-zero mean stress; AW = as-welded; SR = stress relieved; DF = different frequencies; $F = f_{\Sigma}/f_T$).

margin of safety to always be reached when addressing problems of practical interest.

It is possible to conclude by observing that, owing to the intrinsic flexibility of our local approach, structural engineers can follow the same strategy as the one described in Refs [24,64,65] by adopting, according to their in-field experience, different reference curves to calibrate the MWCM as well as to calculate M-D_V in order to more efficiently perform the fatigue assessment of both steel and aluminium weldments.

9. Conclusions

(1). The most important peculiarity of the definitions adopted in the present study and suitable for calculating the stress quantities relative to the critical plane under both CA and VA uniaxial/multiaxial fatigue loading is that they can easily be implemented allowing the design problem to efficiently be addressed numerically.

(2). Independently of the adopted standard stress analysis (i.e., either nominal quantities, hot-spot stresses, or the reference radius idea), the MWCM is seen to be successful in estimating fatigue lifetime of both steel and aluminium weldments subjected to CA as well as to VA uniaxial/multiaxial fatigue loading: accordingly, it is a powerful candidate to be considered for being included amongst those method recommended by the available standard codes.

(3). Even if the TCD based methods are not included in any standard codes or recommendations yet, the MWCM applied in terms of the PM has proven to be highly accurate in estimating fatigue lifetime of steel and aluminium welded joints subjected to either CA or VA fatigue loading: this result is very promising, especially owing to the fact that our method can be applied by directly post-processing simple linear-elastic FE models, i.e., without the need for defining any nominal quantities.

References

[1] Anon. Design of steel structures. ENV 1993-1-1, EUROCODE 3, 1988.
[2] Anon. Design of aluminium structures – Part 2: Structures susceptible to fatigue prENV 1999, EUROCODE 9, 1999.
[3] Hobbacher A. Recommendations for fatigue design of welded joints and components. IIW Document XIII-2151-07/XV-1254-07, May 2007.
[4] Radaj D, Sonsino CM, Fricke W. Fatigue assessment of welded joints by local approaches. Cambridge, UK: Woodhead Publishing Limited; 2007.
[5] Niemi E. Stress determination for fatigue analysis of welded components. Cambridge, England: Abington Publishing; 1995.
[6] Lazzarin P, Tovo R. A notch stress intensity factor approach to the stress analysis of welds. Fatigue Fract Engng Mater Struct 1998;21(21):1089–104.
[7] Lazzarin P, Livieri P. Notch stress intensity factors and fatigue strength of aluminium and steel welded joints. Int J Fatigue 2001;23:225–32.
[8] Lazzarin P, Zambardi R. A finite-volume-energy based approach to predict the static and fatigue behaviour of components with sharp V-shaped notches. Int J Fracture 2001;112:275–829.
[9] Livieri P, Lazzarin P. Fatigue strength of steel and aluminium welded joints based on generalised stress intensity factors and local stain energy. Int J Fracture 2005;133:247–76.
[10] Taylor D, Barrett N, Lucano G. Some new methods for predicting fatigue in welded joints. Int J Fatigue 2002;24:509–18.
[11] Crupi G, Crupi V, Guglielmino E, Taylor D. Fatigue assessment of welded joints using critical distance and other methods. Eng Fail Anal 2005;12:129–42.
[12] Sonsino CM. Multiaxial fatigue assessment of welded joints – recommendations for design codes. Int J Fatigue 2009;31:173–87.

[13] Sonsino CM. Multiaxial fatigue of welded joints under in-phase and out-of-phase local strains and stresses. Int J Fatigue 1995;17:55–70.
[14] Sonsino CM, Kueppers M. Multiaxial fatigue of welded joints under constant and variable amplitude loadings. Fatigue Fract Engng Mater Struct 2001;24:309–27.
[15] Bäckström M, Marquis G. A review of multiaxial fatigue of weldments: experimental results, design code and critical plane approaches. Fatigue Fract Engng Mater Struct 2001;24:279–91.
[16] Lazzarin P, Sonsino CM, Zambardi R. A notch stress intensity approach to assess the multiaxial fatigue strength of welded tube-to-flange joints subjected to combined loadings. Fatigue Fract Engng Mater Struct 2004;27:127–40.
[17] Lazzarin P, Livieri P, Berto F, Zappalorto M. Local strain energy density and fatigue strength of welded joints under uniaxial and multiaxial loading. Eng Frac Mech 2008;75:1875–89.
[18] Palmgren A. Die Lebensdauer von Kugellagern. Verfahrenstechnik 1924;68:339–41.
[19] Miner MA. Cumulative damage in fatigue. J Appl Mech 1945;67:AI59–64.
[20] Gurney T. Cumulative damage of welded joints. Cambridge, England: Woodhead Publishing; 2006.
[21] Sonsino CM. Fatigue testing under variable amplitude loading. Int J Fatigue 2007;29:1080–9.
[22] Kueppers M, Sonsino CM. Assessment of the fatigue behaviour of welded aluminium joints under multiaxial spectrum loading by a critical plane approach. Int J Fatigue 2006;28:540–6.
[23] Sonsino CM, Wiebesiek J. Assessment of multiaxial spectrum loading of welded steel and aluminium joints by modified equivalent stress and Gough-Pollard algorithms. IIW-Doc. No. XIII-2158r1-07/XV-1250r1-07, 2007.
[24] Susmel L. Multiaxial notch fatigue: from nominal to local stress–strain quantities. Cambridge (UK): Woodhead & CRC; 2009.
[25] Lemaitre J, Chaboche JL. Mechanics of solid materials. Cambridge, UK: Cambridge University Press; 1990.
[26] Weber B, Kenmeugne B, Clement JC, Robert JL. Improvements of multiaxial fatigue criteria computation for a strong reduction of calculation duration. Comp Mat Sci 1999;15:381–99.
[27] Bernasconi A. Efficient algorithms for calculation of shear stress amplitude and amplitude of the second invariant of the stress deviator in fatigue criteria applications. Int J Fatigue 2002;24:649–57.
[28] Susmel L, Tovo R, Benasciutti D. A novel engineering method based on the critical plane concept to estimate lifetime of weldments subjected to variable amplitude multiaxial fatigue loading. Fatigue Fract Engng Mater Struct 2009;32:441–59.
[29] Macha E. Simulation investigations of the position of fatigue fracture plane in materials with biaxial loads. Materialwissenschaft und Werkstofftechnik 1989;20:132–6.
[30] Susmel L. A simple and efficient numerical algorithm to determine the orientation of the critical plane in multiaxial fatigue problems. Int J Fatigue 2010;32:1875–83.
[31] Susmel L, Tovo R. Estimating fatigue damage under variable amplitude multiaxial fatigue loading. Fatigue Fract Engng Mater Struct 2011;34:1053–77.
[32] Matsuishi M, Endo T. Fatigue of metals subjected to varying stress. Fukuoka, Japan: Presented to the Japan Society of Mechanical Engineers; 1968.
[33] Susmel L, Tovo R. On the use of nominal stresses to predict the fatigue strength of welded joints under biaxial cyclic loadings. Fatigue Fract Engng Mater Struct 2004;27:1005–24.
[34] Sonsino CM. A consideration of allowable equivalent stresses for fatigue design of welded joints according to the notch stress concept with the reference radii r_{ref} = 1.00 and 0.05 mm. Welding World 2009;53(3–4):R64–75.
[35] Susmel L, Lazzarin P. A bi-parametric modified wöhler curve for high cycle multiaxial fatigue assessment. Fatigue Fract Engng Mater Struct 2002;25:63–78.
[36] Lazzarin P, Susmel L. A stress-based method to predict lifetime under multiaxial fatigue loadings. Fatigue Fract Engng Mater Struct 2003;26:1171–87.
[37] Susmel L, Petrone N. Multiaxial fatigue life estimations for 6082-T6 cylindrical specimens under in-phase and out-of-phase biaxial loadings. In: Carpinteri A, de Freitas M, Spagnoli A, editors. Biaxial and multiaxial fatigue and fracture. Oxford, UK: Elsevier-ESIS; 2003. p. 83–104. ISBN: 0-08-044129-7.
[38] Susmel L, Tovo R, Lazzarin P. The mean stress effect on the high-cycle fatigue strength from a multiaxial fatigue point of view. Int J Fatigue 2005;27:928–43.
[39] Susmel L. Multiaxial fatigue limits and material sensitivity to non-zero mean stresses normal to the critical planes. Fatigue Fract Engng Mater Struct 2008;31:295–309.
[40] Susmel L, Sonsino CM, Tovo R. Accuracy of the modified Wöhler curve method applied along with the r_{ref} = 1 mm concept in estimating lifetime of welded joints subjected to multiaxial fatigue loading. Int J Fatigue 2011;33:1075–91.
[41] Haibach E. Betriebsfestigkeit—Verfahren und Daten zur Bauteilberechnung. Düsseldorf, Germany: VDI-Verlag GmbH; 1989.
[42] Susmel L. Estimating fatigue lifetime of steel weldments locally damaged by variable amplitude multiaxial stress fields. Int J Fatigue 2010;32:1057–80.
[43] Spindel JE, Haibach E. Some considerations in the statistical determination of the shape of S–N cruves. In: Little RE, Ekvall JC. (Eds.), Statistical analysis of fatigue data, ASTM STP 744, 1981. p. 89–113.
[44] Yousefi F, Witt M, Zenner H. Fatigue strength of welded joints under multiaxial loading: experiments and calculation. Fatigue Fract. Engng. Mater. Struct. 2001;24:339–55.
[45] Amstutz H, Storzel K, Seeger T. Fatigue crack growth of a welded tube-flange connection under bending and torsional loading. Fatigue Fract Engng Mater Struct 2001;24:357–68.
[46] Young JY, Lawrence FV. Predicting the fatigue life of welds under combined bending and torsion. Report No. 125, UIL-ENG 86–3602, University of Illinois at Urbana – Champaign, USA, 1986.
[47] Siljander A, Kurath P, Lowrence FV. Non-proportional fatigue of welded structures. In: Mitchell MR, Landgraf R, editors. Advances in fatigue lifetime predictive techniques, ASTM STP 1122. Philadelphia: ASTM; 1992. p. 319–38.
[48] Bäckström M, Siljander A, Kuitunen R, Ilvonen R. Multiaxial fatigue experiments of square hollow section tube-to-plate welded joints. In: Blom AF, editor. Welded high-strength steel structures. London: EMAS; 1997. p. 163–77.
[49] Bäckström M. Multiaxial fatigue life assessment of welds based on nominal and hot spot stresses. VTT PUBLICATIONS 502, VTT Technical Research Centre of Finland, 2003 (ISBN 951-38-6234-8).
[50] Archer R. Fatigue of a welded steel attachment under combined direct stress and shear stress. In: Maddox SJ. (Ed.), Proceedings of fatigue of welded constructions, Brighton, England, 1987. p. 63–72.
[51] Razmijo GR. Fatigue of load-carrying fillet welded joints under multiaxial loading. In: Fatigue: core research from TWI, Woodhead, UK, 2000. p. 63–99, (ISBN 1 85573 520 2).
[52] Maddox SJ, Razmjoo GR. Interim fatigue design recommendations for fillet welded joints under complex loading. Fatigue Fract Engng Mater Struct 2001;24:329–37.
[53] Pyttel B, Grawenhof P, Berger C. (2011) Application of different concepts for fatigue design of welded joints in rotating components in mechanical engineering. Int J Fatigue 2012;34:35–46.
[54] Kueppers M, Sonsino CM. Critical plane approach for the assessment of the fatigue behaviour of welded aluminium under multiaxial loading. Fatigue Fract Engng Mater Struct 2003;26:507–13.
[55] Costa JDM, Abreu LMP, Pinho ACM, Ferreira JAM. Fatigue behaviour of tubular AlMgSi welded specimens subjected to bending-torsion loading. Fatigue Fract Engng Mater Struct 2005;28:399–407.
[56] McDiarmid DL. Fatigue under out-of-phase biaxial stresses of different frequencies. In: Miller KM, Brown MW, (Eds.), Multiaxial Fatigue, ASTM STP 853, American Society for Testing and Materials, Philadelphia, 1985. p. 606–21.
[57] Sines G. Behaviour of metals under complex static and alternating stresses. In: Sines G, Waisman JL, editors. Metal fatigue. McGraw-Hill: New York; 1959. p. 145–69.
[58] Davoli P, Bernasconi A, Filippini M, Foletti S, Papadopoulos IV. Independence of the torsional fatigue limit upon a mean shear stress. Int J Fatigue 2003;25:471–80.
[59] Haibach E. Service fatigue-strength – methods and data for structural analysis. Germany, VDI: Düsseldorf; 1992.
[60] Susmel L, Tovo R. Local and structural multiaxial stress states in welded joints under fatigue loading. Int J Fatigue 2006;28:564–75.
[61] Tovo R, Lazzarin P. Relationships between local and structural stress in the evaluation of the weld toe stress distribution. Int J Fatigue 1999;21:1063–78.
[62] Radaj D. Review of fatigue strength assessment of nonwelded and welded structures based on local parameters. Int J Fatigue 1996;18:153–70.
[63] Sonsino CM, Bruder T, Baumgartner J. SN-curves for welded thin joints – suggested slopes and fat-values for applying the notch stress concept with various reference radii. IIW-Doc. No. XIII-2280 (2009)/XV-1325, 2009.
[64] Susmel L. Modified Wöhler curve method, theory of critical distances and EUROCODE 3: a novel engineering procedure to predict the lifetime of steel welded joints subjected to both uniaxial and multiaxial fatigue loading. Int J Fatigue 2008;30:888–907.
[65] Susmel L. The modified Wöhler curve method calibrated by using standard fatigue curves and applied in conjunction with the theory of critical distances to estimate fatigue lifetime of aluminium weldments. Int J Fatigue 2009;31:197–212.
[66] Maddox SJ. Review of fatigue assessment procedures for welded aluminium structures. Int J Fatigue 2003;25:1359–78.
[67] Morgenstern C, Sonsino CM, Hobbacher A, Sorbo F. Fatigue design of aluminium welded joints by the local stress concept with the fictitious notch radius of r_f = 1 mm. Int J Fatigue 2006;28:881–90.